Whole Virion Proteomics of HCMV Reveals that gpUL141 is a Virion Component that Regulates Envelope Glycoprotein Composition to Protect Against Humoral Immunity

Kirsten Bentley[1]#, Evelina Statkute[1]#, Isa Murrell[1]#, Ceri Fielding[1], Robin Antrobus[2], Hannah Preston[1], Lauren Kerr-Jones[1], Daniel Cochrane[1], Ilija Brizic[3], Paul J. Lehner[4], Gavin Wilkinson[1], Eddie Wang[1], Stephen C. Graham[5], Michael P. Weekes[2], Richard J. Stanton[1]*

*Corresponding Author, StantonRJ@cardiff.ac.uk

#These authors contributed equally

1. Infection and Immunity, Cardiff University School of Medicine, Cardiff, CF14 4XN

2. Cambridge University Institute for Medical Research, Cambridge University, Cambridge CB2 0XY

3. School of Medicine, University of Rijeka, Rijeka, Croatia

4. Cambridge Institute for Therapeutic Immunology and Infectious Disease, Cambridge University, Cambridge

5. Department of Pathology, University of Cambridge, Cambridge, CB2 1QP

Abstract

Human cytomegalovirus (HCMV) is a clinically important herpesvirus that has co-evolved for millions of years with its human host, and establishes lifelong persistent infection. A substantial proportion of its 235kb genome is dedicated to manipulating host immunity through targeting antiviral host proteins for degradation or relocalisation. Quantitative proteomics of the infected cell has extensively characterised these processes, but the cell-free virion has been less well studied. We therefore carried out proteomic analysis of a clinical HCMV strain virion. This revealed multiple novel components, including the viral protein gpUL141, which is recognised as an NK immune-evasin that targets several host proteins (CD155, CD112, and TRAILR) when expressed in the cell. Co-Immunoprecipitation of gpUL141 from virions identified interactions with viral entry glycoproteins from the trimer (gH/gL/gO), pentamer (gH/gL/UL128/UL130/UL131A), and gH/gpUL116 complexes, as well as gB. These interactions occurred via direct interactions between gpUL141 and either gH or gB. Analysis supported a model in which gpUL141 homodimers independently interacted with separate gB/gH-containing complexes. gpUL141 encodes an ER retention domain that restricts trafficking through the ER/golgi, and limited the transport of glycoprotein complexes bound by gpUL141. As a result, gpUL141 reduced levels of multiple glycoprotein complexes on the infected cell surface as well as in the virion. This reduced syncytia formation, inhibited antibody-dependent cellular cytotoxicity (ADCC), and reduced susceptibility to neutralising antibodies. Thus, gpUL141 represents an immune-evasin that not only targets host proteins to limit NK-cell attack, but also alters the trafficking of multiple viral glycoprotein complexes in order to evade humoral immunity.

Significance

The large number of immune-evasins encoded by HCMV has led to it becoming a paradigm for pathogen-mediated immune-modulation. These mechanisms have informed on virus pathogenesis, revealed the underlying function of human immunology, and identified therapeutic targets. Previously discovered immune-evasins functioned by modifying host proteins, gpUL141 represents a novel strategy in which multiple immunological functions are targeted through manipulating eight different viral entry glycoproteins, via interactions with two proteins common to multiple complexes. Entry glycoproteins define virus tropism, mechanisms of infection and spread, and susceptibility to neutralising and non-neutralising antibody activities, yet UL141 is frequently mutated in passaged HCMV strains. Since vaccines and immunotherapies exploit these functions, it is critical that gpUL141 activity is accounted for when assessing preclinical efficacy.

Introduction

Human cytomegalovirus (HCMV) is a clinically significant betaherpesvirus that establishes lifelong persistence in the majority of people worldwide. It is a significant cause of morbidity and mortality in the immunocompromised, and the leading infectious cause of congenital malformation. To date, no vaccine is licensed, and antivirals are limited by toxicity and the selection of resistance mutations.

HCMV has the largest genome of any human virus and has co-evolved with its human host for many millions of years. This has enabled it to develop an exceptionally broad range of mechanisms to manipulate host immunity to promote persistence. Only 41-45 of the 170 canonical ORFs are essential for replication *in vitro*, with the remainder providing accessory functions required *in vivo*[1,2]. These include proteins that prevent cell death, inhibit innate and intrinsic immunity, limit T-cell recognition, and prevent NK-cell attack, through targeting host antiviral proteins for degradation or relocalisation[3-5]. As a result of these activities, HCMV has become a paradigm for pathogen-mediated immune-evasion.

A challenge of studying these viral accessory functions in HCMV is that mutations in non-essential genes are invariably selected when clinical viruses are passaged *in vitro*. Although the loss of a 15kb genetic region encoding >20 genes in the AD169 strain is the most extreme example, even short-term passage rapidly selects for mutations[6]. As a result, laboratory strains differ both genotypically and phenotypically from the causative agent of disease[7]. To address this problem, we previously generated an infectious bacterial artificial chromosome (BAC) clone of a HCMV strain (Merlin) for which we had the sequence of the original clinical material[7,8]. This allowed us to correct *in vitro* acquired mutations and re-generate virus containing a genome that exactly matched the patient sample. Like clinical isolates, this virus also accrued mutations upon passage *in vitro*, with RL13 and a complex of three genes, UL128, UL130, UL131A (the UL128 locus; UL128L), the most rapidly selected. Engineering of the Merlin BAC enabled us to selectively repress these genes when virus stocks were grown *in vitro*, permitting recovery of high titre virus for experimental use without risk of mutation.

Study of strain Merlin has led to the discovery of multiple phenomenon which differ between passaged and clinical viruses, including extensive virus-induced modulation of the cell-surface proteome through metalloproteinase manipulation[9], novel cell-surface therapeutic targets[10], immune-evasion mediated by actin manipulation[11], functions that prevent Natural Killer cell attack[12-14], and mechanisms that promote a form of cell-associated spread that is highly resistant to neutralising antibodies[8,15]. Many of these discoveries were underpinned by extensive use of quantitative proteomics analysis to understand how HCMV manipulates the infected cell to drive viral survival following entry[16-27]. However, the virion itself has not been subject to the same level of investigation. Previous mass spectrometry analyses have been carried out using the passaged AD169[28] and TB40[29] strains. However, given the existence of mutations in these strains, we carried out an analysis of virions derived from the Merlin BAC with the intention of producing a wildtype HCMV virion proteome. We unexpectedly discovered that glycoprotein UL141 (gpUL141) is a novel virion component. Although previously demonstrated to manipulate host ligands (CD155, CD112, and TRAILR) to limit NK activation[12-14], we now show that it has also been co-opted by HCMV to manipulate the trafficking of the majority of viral entry glycoproteins to the cell surface and the virion particle in order to provide resistance to multiple different aspects of humoral immunity.

Results

The wildtype HCMV virion contains multiple proteins absent from passaged strains

To define the complete repertoire of proteins associated with the strain Merlin virion, we used mass spectrometry to analyse virions that had been separated from non-infectious particles and dense bodies on glycerol-tartrate gradients. We individually analysed six Merlin variants that we were working with as part of previous studies: a wildtype genome, a genome mutated for RL13, and a genome mutated for both RL13 and UL128L, to assess alterations deriving from the presence or absence of the pentameric complex and/or gpRL13[8]; two viruses were included that contained point mutations in an intron of UL128 that result in intermediate UL128L expression levels enabling comparisons with passaged strains of HCMV that retain pentamer expression but at lower levels[30]; and a virus lacking UL141[13]. In addition to analysing virion preparations individually, quantitative comparisons were made by producing virions in media containing different isotopes of arginine and lysine (Stable Isotope Labelling of Amino Acids in Culture; SILAC), then analysing as two groups of three variants (Fig 1A, Table S1).

These SILAC analyses of near identical Merlin virions, differing only in RL13 and UL128L, indicated that deletion of RL13 made very little difference to the relative abundance of virion proteins while loss of UL128L led to higher levels of gO (as previously reported)[30,31] and UL146 (Figure S1). Aside from this, there were no consistent differences that would support effects of these proteins on other virion components. The absolute Merlin virion proteome was determined as the consensus of proteins identified across all virion preparations. 96 viral proteins were designated as 'high confidence' when the peptides were present in at least half of all virus preparations (Table 1). Of these, 53 were previously identified by mass spectrometry analysis of AD169 virions[28], and 35 by mass spectrometry analysis of TB40[29]. A further nine proteins not identified by mass spectrometry analysis of AD169 or TB40 virions, but recognised as HCMV virion components following assessment of virions by alternative approaches, were also detected with high confidence (UL36, RL11[32], gpRL13[8], gpUL130[33,34], gpUS28[35], gpUL116[36],UL148[37], UL23[38], and UL114[39].

31 proteins identified with high confidence have not been previously described as virion components. Of these, 6 are implicated in viral genome transcription/replication and virion assembly and 13 are membrane-localised. Some of these proteins have been found as virion components in CMVs from other species, for example homologous proteins to pUL52 (Rh83), gpUL141 (Rh164), and pUS12 (Rh190) have been identified in RhCMV virions, whilst homologous proteins of pUL70 (M70) have also been identified in MCMV virions, however others are unique to HCMV (Table 1).

We used iBAQ (intensity-based absolute quantitation) values for virions with a wild-type genome to estimate the relative abundance of different virion components. Certain proteins accounted for a substantial overall proportion of the total protein content of the virion. These included tegument proteins pp65 (~43%), pp71 (~4%) and pp150 (~1.5%) as well as capsid proteins UL86 (~5%) and UL85 (~4%). To determine which viral components were specifically enriched in the virion in contrast to lysates of infected cells, we compared iBAQ values for virion proteins with those we previously calculated for cells infected with Merlin-strain HCMV[22]. Most proteins exhibited similar abundance, but there was a 2-340 fold enrichment of multiple virion membrane proteins, as well as capsid and tegument proteins. These included membrane proteins gN, gM, gH and gL, capsid proteins UL46, UL47 and UL85 as well as tegument proteins UL83, UL82 and UL103 (Fig. S2A-B, Table S2A). There was also enrichment of certain types of cellular proteins,

particularly those with transmembrane domains, lipoproteins, ATP synthase subunits and host receptors for viral entry. The latter included known receptors for HCMV including Integrins β1 and α2 (Figure S3A-B, Tables S2B-C).

Table 1. Virus encoded proteins identified by MS-analysis of Merlin virions.

ORF[a]	Rank[b]	ID[c]	Protein/Function[d]	AD169[e]	RhCMV[f]	MCMV[g]	TB40[h]
A- Proteins identified with high confidence							
Capsid:							
UL46	8	8/8	pUL46/mCBP (minor capsid protein binding protein); interacts with mCP to form capsid triplex	X	X	X	X
UL48A	17	8/8	pUL48A/SCP (smallest capsid protein); decorates capsid hexons	X	X	X	X
UL80	39	8/8	pUL80/PR-AP (assembly protein) precursor; scaffold for capsid assembly	X	X	X	X
UL85	6	8/8	pUL85/mCP (minor capsid protein); interacts with mCBP to form capsid triplex	X	X	X	X
UL86	3	8/8	pUL86/MCP (major capsid protein); forms capsid walls and faces	X	X	X	X
UL104	70	8/8	pUL104/PORT; forms specialized portal capsomere for genome insertion/release	X	X	X	X
Tegument:							
UL23	67	6/8	Tegument. Inhibits transcription of IFN-γ stimulated genes				
UL24	19	8/8	pUL24; US22 family member; enhances replication in endothelial cells	X	X		X
UL25	7	8/8	pUL25; UL25 family member	X	X	X	X
UL26	16	8/8	pUL26; US22 family member, MIEP transcription transactivator, tegument material phosphorylation, stabilises virion	X	X		
UL28/UL29	79	5/8	pUL28/UL29; US22 family member, Stimulates IE gene expression			X	
UL32	12	8/8	pp150 / NSP (nucleocapsid-proximal stabilization protein); virion maturation	X	X	X	X
UL35	41	8/8	pUL35; UL25 family member, virion morphogenesis	X	X	X	X
UL36x1	50	7/8	pUL36x1; US22 family member, vICA (viral inhibitor of caspase-8-induced apoptosis)				
UL43		8/8	pUL43; US22 family member	X		X	
UL45	15	8/8	pUL45/RR1 (Ribonucleotide reductase homologue sub-unit)	X	X	X	X
UL47	28	8/8	pUL47/LTPbp (Largest tegument protein binding protein); interacts with ppUL48 intra-cellular transport of nucleocapsid	X	X	X	X
UL48	33	8/8	pUL48/LTP (Largest tegument protein); interacts with ppUL47 intra-cellular transport of nucleocapsid	X	X	X	X

UL50	38	8/8	pUL50/NEC1 (nuclear egress complex membrane anchoring component 1); interacts with pUL53 (NEC2) to orchestrate nuclear egress of nucleocapsids	X	X		
UL52	62	8/8	pUL52; DNA encapsidation, nucleocapsid formation		X		
UL69	49	8/8	ppUL69; MRP (multiple regulatory protein)	X		X	X
UL71	47	8/8	pUL71; Secondary envelopment, virion egress	X	X	X	X
UL82	5	8/8	ppUL82/pp71/UMP (upper matrix protein); secondary envelopment, relieves DAXX-mediated repression	X	X	X	X
UL83	1	8/8	ppUL83/pp65/LMP (lower matrix protein); phosphorylase, innate and adaptive immune response evasion	X	X	X	X
UL88	34	8/8	pUL88; Putative cytoplasmic egress function	X	X	X	X
UL94	11	8/8	pUL94; interacts with pp28 to facilitate secondary envelopment	X	X	X	X
UL96	76	7/8	pUL96; interacts with pp150 to stabilise nucleocapsid during cytoplasmic egress	X	X		
UL97	35	8/8	ppUL97/VPK (viral protein kinase); phosphorylates viral and cellular proteins	X	X	X	X
UL99	20	8/8	ppUL99/pp28; myristylated protein, secondary envelopment	X	X	X	X
UL103	54	7/8	pUL103; VEP (Virion and DB egress protein); orchestrates release from producer cells	X	X		
IRS1	18	8/8	pIRS1; US22 family member, PKR (Protein kinase R) inhibitor, Transcriptional activator	X			
US22	32	8/8	pUS22; US22 family member	X	X	X	
US23	91	8/8	pUS23; US22 family member	X			
US24	82	7/8	pUS24; US22 family member; enhances early infection	X	X		
TRS1	85	8/8	pTRS1; US22 family member, PKR (Protein kinase R) inhibitor, Transcriptional activator, capsid assembly	X	X		
Transcription/replication machinery, yet to be assigned to virion compartment:							
UL34	57	8/8	pUL34; Represses US3 transcription				
UL44	2	8/8	ppUL44/PPS (Viral DNA polymerase processivity sub-unit); DNA synthesis	X	X	X	
UL57	55	8/8	ppUL57/SSB (single-stranded DNA binding protein); DNA synthesis	X		X	
UL70	73	8/8	pUL70/HP2 (DNA helicase-primase sub-unit 2); DNA synthesis			X	
UL77	72	8/8	pUL77/CVC1 (putative capsid vertex-specific component 1); DNA encapsidation	X	X	X	
UL84	24	8/8	ppUL84/Viral DNA replication accessory; DURP family member, DNA synthesis	X	X		

UL89	60	8/8	pUL89/TER1 (terminase sub-unit 1); DNA encapsidation	X			X
UL93	83	7/8	pUL93/CVC2 (putative capsid vertex-specific component 2); DNA encapsidation	X	X		X
UL98	44	8/8	pUL98/NUC (deoxyribonuclease)		X	X	
UL112-UL113	40	8/8	pUL112/UL113; Orchestrates DNA synthesis, transcriptional activator	X	X		
UL114	59	7/8	ppUL114; DNA synthesis UNG (Uracil-DNA glycosylase), control DNA synthesis				
UL122	48	8/8	pUL122; IE2; transactivator or host-cell transcription machinery	X	X		X
UL146	66	7/8	gpUL146; vCXC chemokine homologue family, putative chemokine				
UL54	81	5/8	pUL54; POL; catalytic DNA polymerase sub-unit	X		X	
UL56	86	6/8	pUL56; TER2 (terminase sub-unit 2); DNA encapsidation	X		X	
UL102	87	5/8	pUL102/HP3 (helicase primase sub-unit 3); DNA synthesis		X	X	
UL147	69	6/8	pUL147; vCXC-2 chemokine homologue family, putative chemokine				
Envelope:							
RL10	29	8/8	gpRL10	X			X
RL11	51	8/8	gpRL11/gp34; RL11 family member, IgG Fc binding				
RL12	25	8/8	gpRL12/gp95; RL11 family member, IgG Fc binding				
RL13	23	2/2	gpRL13; RL11 family member, putative IgG Fc binding, impedes replication in fibroblasts and epithelial cells		X		
UL16	30	7/8	gpUL16; membrane glycoprotein, NK cell evasion, blocks NKG2D ligands MICB, ULBP1 and ULBP2				
UL33x1	43	8/8	pUL33x1; GPCR homologue family member, constitutive signalling GPCR	X	X		X
UL37	53	5/8	Isoform vMIA of pUL37; multifunctional transmembrane protein that plays several key roles in viral replication				
UL41A	31	7/8		X	X		X
UL55	13	8/8	gB; gCI subunit, virion binding and entry	X	X	X	X
UL73	21	8/8	gN; gCII sub-unit, virion binding, progeny virion secondary envelopment	X	X		
UL74	92	8/8	gO; gCIII sub-unit, fibroblast cell entry, release of progeny virions from producer cells	X	X	X	
UL74A	58	6/8	gpUL74A; putative membrane glycoprotein				

UL75	37	8/8	gH; gCIII/pentameric complex sub-unit, entry into cells	X	X	X	
UL78	74	8/8	gpUL78; GPCR homologue family member; putative chemokine receptor				
UL100	87	8/8	gM; gCII sub-unit, virion binding, progeny virion secondary envelopment	X	X	X	X
UL115	52	7/8	gL; gCIII/pentameric complex sub-unit, entry into cells	X	X		
UL116	42	8/8	gpUL116; putative membrane glycoprotein		X		
UL118-UL119	78	8/8	gpUL118-UL119/gp68; IgG Fc binding	X	X		X
UL128	45	5/6	gpUL128; pentameric complex, entry into non-fibroblasts				X
UL130	63	5/6	gpUL130; pentameric complex, entry into non-fibroblasts				
UL131A	75	6/6	gpUL131A; pentameric complex, entry into non-fibroblasts				X
UL132	10	8/8	gpUL132; enhances replication in fibroblasts	X	X		X
UL139	94	5/8	gpUL139; putative membrane glycoprotein				
UL140	95	6/8	pUL140; putative membrane protein				
UL141	9	7/7	gpUL141; UL14 family member, NK evasion, down regulates CD155 and CD112		X		
UL148	14	7/8	gpUL148, putative membrane glycoprotein				
US9	46	7/8	gpUS9; US6 family member, membrane glycoprotein				
US12	65	8/8	pUS12; US12 family member, 7TM protein		X		
US13	77	6/8	pUS13; US12 family member, 7TM protein				
US14	80	8/8	pUS14; US12 family member, 7TM protein				
US20	27	8/8	pUS20; US12 family member, 7TM protein				
US27	26	8/8	gpUS27; GPCR homologue family member, 7TM protein, enhances virion release	X			X
US28	56	8/8	gpUS28; GPCR homologue family member, 7TM protein, CC and CXC3 chemokine receptor		X		
Uncharacterised:							
RL1	68	5/8	pRL1; RL1 family member, Degrades the host antiviral factor SLFN11 via the cullin4-RING E3 ubiquitin ligase (CRL4) complex				
UL13	88	6/8	pUL13; modulates mitochondrial ultrastructure		X		
UL31	90	7/8	pUL31; DURP family member			X	

UL95	89	7/8	Participates in the expression of late viral mRNAs			X	
UL135	97	5/8	pUL135; reactivation from latency, actin remodelling				
UL145	22	7/8	pUL145; recruit DDB1-containing ubiquitin ligases to induce proteasomal degradation of STAT2.				
UL148D	36	6/8	Inhibits ADAM17 function				X
UL150A	71	6/8	Putative secreted protein				
US1	84	7/8	US1 family member		X		
US8	61	7/8	gpUS8; Type I membrane glycoprotein				
US26	93	6/8	pUS26; US22 family member		X		
B- Proteins identified with low confidence							
Transcription/replication machinery, immune evasions, yet assigned to virion compartment:							
UL105		4/8	pUL105; HP1 (helicase-primase sub-unit 1), DNA synthesis			X	
UL123		4/8	ppUL123/IE1 (major IE protein); promotes transcription cascade, enhances IE2 activation				
Envelope:							
UL15A		1/8	Uncharacterised				
UL40		2/8	Loads peptides onto HLA-E				
US3		4/8	Retains MHC class I heterodimers in the endoplasmic reticulum				
US18		4/8	pUS18; US12 family member, 7TM protein		X		
Uncharacterised							
RL9A		1/8					
UL5		2/8	May play a role in rearrangement of cellular cytoskeleton towards an efficient viral assembly and spreading.	X			
UL14		4/8	Uncharacterised				
UL17		3/8					
UL22A		3/8	Glycoprotein	X			
UL27		1/8	Uncharacterised				

UL30	1/8	Uncharacterised		X	
UL49	4/8	pUL49; subunit of the viral pre-initiation complex, regulates gene transcription	X		
UL53	4/8	pUL53 (NEC2) (nuclear egress complex membrane anchoring component 2); interacts with pUL50/NEC1 to orchestrate nuclear egress of nucleocapsids			
UL72	2/8	Deoxyuridine 5-triphosphate nucleotidohydrolase	X		X
UL76	4/8	pUL76; modulates gene expression			
UL117	1/8	Plays a role in the inhibition of host DNA replication in the infected cell			
UL136	1/8	Plays a role in latency			
UL138	3/8	Modulates the expression of several host cell surface receptors			
UL150	1/8	Uncharacterised			
US30	1/8	Uncharacterised			
US32	4/8	Uncharacterised			

[a] ORFs encoding proteins identified in Merlin virions.
[b] rank of protein based on abundance in the wildtype HCMV virion proteome, with 1 being the most abundant as assessed by IBAQ.
[c] identities depict the number of virion preparations in which proteins were detected.
[d] comments as to the biochemistry and function of proteins identified, as described in Field's Virology
[e] proteins previously identified during mass spectrometry analysis of HCMV Strain AD169 virions[28]
[f] homologous proteins identified during mass spectrometry analysis of RhCMV virions[40]
[g] homologous proteins identified during mass spectrometry analysis of MCMV virions[41]
[h] homologous proteins identified during mass spectrometry analysis of HCMV Strain TB40 virions[29]

gpUL141 is a novel virion envelope glycoprotein, but does not act as an immune-evasin when delivered by the virion

We have previously characterised the viral protein gpUL141 as a potent inhibitor of NK activation. When expressed within the cell, it binds CD155 and all four TRAIL receptors and prevents surface expression by retaining them within the ER[12,14]. This has the effect of rendering cells more resistant to TRAIL-mediated apoptosis and NK-cell attack. It also co-operates with US2 to target CD112 for degradation, preventing NK-cell activation[13,17]. We were therefore interested to note that our proteomics analysis identified gpUL141 as a novel virion component that has not previously been identified as such because many widely used HCMV strains have *in vitro* selected mutations that abrogate UL141 expression[6,42]. Western blot analysis confirmed the presence of gpUL141 in purified virions in the absence of its cellular ligand CD155 (Fig 1B). Fractionation of virions confirmed that it was in the envelope compartment (Fig 1C), consistent with the fact that it encodes a transmembrane domain and a signal peptide. Interestingly gpUL141 found in the virion was resistant to EndoH, while cell-associated gpUL141 was sensitive (Fig 1D), suggesting that gpUL141 is present as two fractions – one is retained within the ER within the cell, while the other must traffic through the ER and the Golgi to be incorporated into the virion.

Given the characterised role of gpUL141 as an immune-evasin, we investigated whether virion-delivered gpUL141 could act as a rapid immune-evasin, prior to *de novo* gene expression. Cells were infected with wildtype HCMV or HCMV lacking UL141, either as live or irradiated virus. Cells were then co-cultured with NK cells and NK-degranulation assessed. 2h post-infection, neither the presence or absence of UL141, nor the ability of the virus to initiate *de novo* gene expression, had any impact on NK activation (Fig 1E). At 24h post-infection, loss of UL141 led to increased NK activation, but this was not seen in the irradiated virus (Fig 1F). Thus, this effect was due to newly-synthesised gpUL141 within the cell. We therefore concluded that virion delivered gpUL141 does not impact NK cell activity, only gpUL141 expressed within the cell has this property.

gpUL141 interacts with multiple HCMV entry glycoproteins within the virion

To determine what other roles virion-associated gpUL141 might play, we carried out a SILAC-immunoprecipitation (SILAC-IP) in which gpUL141 was pulled down via a C-terminal V5 tag from purified virions, then analysed by MS, to identify interacting proteins. We used a virus lacking pentamer expression due to the higher cell-free titres it produces, with analysis revealing interactions of gpUL141 with gB, gH, gL, gO, and gpUL116 (Fig 2A, Table S3). gB is the conserved herpesvirus fusogen, gH/gL/gO form the 'Trimer' complex which is essential for cell-free entry into all cell types via interactions with PDGFRa as well as other (unidentified) receptors[43,44], while gpUL116 interacts with gH but has no known receptor binding role currently[36,45,46]. All interactions were confirmed by IP-western of gpUL141 from purified virions (Fig 2B). Thus, gpUL141 interacts with multiple members of the HCMV entry machinery within the virion.

To determine which interactions with gpUL141 were direct, gpUL141 was expressed from an Adenovirus vector along with each protein from the SILAC-IP individually, then immuno-precipitated. Only gH and gB were robustly co-immunoprecipitated with UL141 in this pairwise test, indicating a direct interaction. Although some interaction was observed with gL, this was significantly weaker than when gH and gL were co-expressed, indicating only a weak interaction. All other proteins are presumably pulled down via indirect interactions (Fig 2C). Consistent with this, when all proteins were expressed together from an Adenovirus vector, all co-

immunoprecipitated with gpUL141, indicating that no other viral proteins are required for all complexes to form (Fig 2D).

Deep learning structure prediction using AlphaFold3 (AF3)[47] was user to further understand the potential physical interactions between gpUL141 and gH or gB. Previous structural characterisation of gpUL141 has indicated that it forms a head-to-tail homodimer when in complex with its cellular targets CD155 or TRAILR2[48,49], hence two copies of the gpUL141 sequence were included in all structure predictions. AF3 predicted a high confidence interaction between gH and the gpUL141 dimer, with gpUL141 contacting domains DI, DII and DIII of gH (Fig 3A, Fig S4). AF3 did not predict a high confidence interaction between gpUL141 and gB (Fig. S4), potentially because AF3 predictions yielded a post-fusion conformation of gB rather than the pre-fusion complex likely to predominate in HCMV virions.

gpUL141 interacts independently with all major gH-containing glycoprotein complexes

HCMV encodes three gH-containing complexes – trimer (gH/gL/gO), pentamer (gH/gL/UL128/UL130/UL131A), and UL116 (gH/UL116) – which are mutually exclusive; UL128 and gO compete for the same binding sites on gL[50], while gL competes with UL116 for binding to gH[36]. The AF3-predicted binding of gpUL141 would not be expected to inhibit the interaction between gH and either gL or gpUL116 (Fig 3B, Fig S4), consistent with our immunoprecipitation experiments, implying that gpUL141 interacts with both gpUL116 and the trimer via gH. This structural model would also imply that gpUL141 could in addition interact with pentamer via gH (Fig 3B). Indeed, when gpUL141 was immunoprecipitated from infected cells, it pulled down UL116, gO, and UL128, indicative of interactions with all recognised gH containing complexes (Fig 3C).

The predicted gpUL141:gH structure is consistent with dimers of gpUL141 symmetrically binding two gH molecules. In this case it could potentially 'bridge' different gH complexes (Fig. S4). To determine whether this occurs we immunoprecipitated gO, then stained for gpUL116 or UL128. Whereas immunoprecipitation of UL141 pulls down all of these proteins (Fig 2B/3C), pulling down gO did not pull down gpUL116 or UL128 (Fig 3D). Similarly, pulling down gpUL116 did not co-precipitate gO (Fig 3E). Therefore, gpUL141 interacts with all three gH containing complexes (Trimer, Pentamer, and gpUL116), but does not link different complexes together. In contrast, the predicted gH binding interface of gpUL141 overlaps significantly with the surface bound by TRAIL-R2 (Fig 3A), suggesting that binding of gpUL141 to gH (and complexes thereof) and TRAIL death receptors would be mutually exclusive, consistent with virion SILAC-IP data (Fig 2A) and western blot (Fig 1B).

gpUL141 modulates cell-surface and virion gH-complex levels

We have previously shown that knocking gpUL141 out of the virus genome has no impact on virus growth in fibroblasts, but enhances growth in epithelial cells[42]. This phenomenon was not restricted to epithelial cells (Fig 4A), virus dissemination was also enhanced in the absence of UL141 in endothelial cells (Fig 4B), suggesting that it occurs in all cell-types where entry is dependent on pentamer. Since gpUL141 can inhibit virus growth and interacts with multiple gH-containing complexes that are required for virus infection, we investigated whether these phenomenon were linked. The majority of gpUL141 is retained within the ER where it prevents transit of CD155 and TRAILR2 through the ER-Golgi apparatus [12,14], yet our data also indicated that virion envelope glycoproteins must traffic through the ER and Golgi in order to become incorporated in the virion envelope (Fig 4C). We therefore investigated whether the gpUL141 retained in the ER also bound gH-containing complexes and affected their transition through the

ER/Golgi. We took advantage of the fact that gO is highly glycosylated, and therefore trafficking from the ER through to the Golgi can be assessed by measuring sensitivity to EndoH. When epithelial cells were infected with HCMV lacking UL141 there was a significant fraction of EndoH resistant gO, which was reduced in virus expressing UL141, indicating that more gO is retained in the ER in the presence of gpUL141 (Fig 4C).

Although we had investigated this phenomenon in epithelial cells due to the growth restriction observed in this cell type, there was no reason to assume that it was restricted to epithelial cells. In support of this, when a comparable assay was carried out in fibroblasts, a similar result was obtained (Fig 4D). We therefore expanded this result by measuring cell-surface levels of gH and gB by flow cytometry in fibroblasts. At 72h post-infection in the presence of gpUL141, gH and gB levels were low (gB) or undetectable (gH). However, when UL141 was deleted, surface levels of gH and gB were enhanced (Fig 4E). Antibodies are not available to detect the cell-surface forms of other gH-containing complexes. To determine whether this phenomenon extended to all proteins that interact either directly or indirectly with gpUL141, we therefore used our previously validated 'Plasma Membrane Profiling' technique to isolate cell-surface proteins and assess levels by western blot[16,51]. In support of EndoH and flow analysis, levels of gO, gH, gL, gpUL116, gB, and UL128 on the plasma membrane were all reduced in the presence of gpUL141, while a control protein (free heavy chains of MHC-B/C) was unaffected (Fig 4F). This phenomenon could also be recapitulated outside of the context of infection, using Adenovirus vectors expressing individual glycoproteins (Fig 4G). When gH is expressed in isolation it does not traffic to the plasma membrane, but it becomes surface-localised when co-expressed with gL, and this is enhanced when gpUL116 is additionally co-expressed. However, in all cases, co-expression of UL141 resulted in a reduction in cell-surface levels. This was dose-dependent, with an excess of UL141 leading to almost complete inhibition of surface trafficking.

Since cell-surface trafficking was altered in the presence of gpUL141, we wondered whether this would also affect the levels of gH-containing complexes found in purified virions. Indeed, in the input samples used for our virion IP-western (Fig. 2B), the levels of proteins from all complexes were all significantly lower in the presence of gpUL141, with the potential exception of gB. Since the effects of gpUL141 on virus growth were more extensive in epithelial cells, we also tested a subset of proteins in virus derived from this cell type. As in fibroblasts, the levels of proteins that interacted directly or indirectly with gpUL141 were reduced within the virion (Fig 3H). Thus, gpUL141 acts to reduce the incorporation of all gH containing complexes into virions, and limits presentation of these complexes (along with gB), on the plasma membrane of the infected cell.

gpUL141 expression limits syncytia formation

Viral entry glycoproteins on the infected cell surface can engage with entry receptors on surrounding cells leading to fusion and the formation of syncytia. In the case of HCMV, this requires gH/gL complexes and gB[52,53]. We reasoned that if all of these were reduced on the infected cell surface, this could reduce receptor engagement and therefore the chances of syncytia formation. ARPE19 epithelial cells have previously been reported to readily form syncytia upon HCMV infection[53]. These cells were therefore infected with GFP-expressing HCMV, and virus allowed to disseminate. No syncytia were observed in the first 3-5 days after infection, however by day 6 a clear difference was observed, with virus lacking gpUL141 expression demonstrating a significant increase in the formation of large multi-nucleated cells (Fig 5). In contrast, these were much rarer in cells infected with wildtype HCMV. Furthermore, the size of syncytia were much lower when gpUL141 was expressed as compared to the virus lacking

expression. Thus, gpUL141 inhibits syncytia formation in epithelial cells, consistent with gpUL141-mediated reduction in cell-surface levels of gH/gL complexes and gB.

gpUL141-mediated modulation of gH-complex levels is due to its ER retention domain, and inhibits humoral antiviral functions

UL141 is retained within the ER where it prevents ER-exit of CD155 and TRAILR[12,14]. It has previously been assumed that this ER-retention function is necessary to prevent cell-surface trafficking of these cellular proteins in order to prevent activation of NK cells. However, our data implies that the ER retention function may have additional impacts on multiple viral entry glycoproteins. For transmembrane proteins, the ER retention domain is often in the C-terminus of the protein, with the classical sequence being KKXX. UL141 contains such a motif at its extreme C-terminus. To explore this further, we therefore generated HCMV viruses in which the C-terminal intracellular portion of UL141 was deleted. We have previously shown that this results in increased trafficking of gpUL141 through the ER/Golgi when expressed from a RAd[10], however surprisingly it did not inhibit the ability of RAd expressed gpUL141 to reduce cell surface levels of CD155, with levels actually down-regulated to a greater extent when the ER retention domain was deleted (Fig 6A). Similarly, when we engineered this mutation into HCMV, it did not alter the ability of gpUL141 to limit cell-surface levels of CD155, TRAILR2, or CD112 (Fig 6B). Therefore, the ability of UL141 to act as a NK-evasin does not require UL141 to be ER-resident.

To determine whether the ER retention domain affected gH-complex trafficking, we repeated the EndoH analysis of gO. In both fibroblast (Fig 6C) and epithelial cells (Fig 6D), loss of the ER retention domain led to an increase in levels of EndoH resistant gO, although not always to the level seen following complete UL141 deletion. When we assessed cell-surface trafficking of gH and gB, removal of the ER retention domain led to recovery of both proteins on the plasma membrane (Fig 6E). Cell-surface viral antigens are a target for humoral immunity, with opsonised HCMV infected cells susceptible to NK-mediated attack through antibody-dependent cellular cytotoxicity (ADCC). Antibodies capable of mediating ADCC against gB or gH-containing complexes have not been described, therefore to determine whether greater trafficking of antigens to the cell surface can enhance susceptibility to ADCC, we tested levels of ADCC induced by antibodies that we have previously isolated against gpUL141 itself. ADCC was significantly enhanced by the greater cell-surface trafficking that arose from loss of the ER retention domain on UL141 (Fig 6F).

To determine whether the ER retention domain also altered the growth properties of virus, we assessed cell-free titers of virus in epithelial cells. As previously, complete loss of UL141 led to higher cell-free titers, and this was phenocopied by the loss of just the ER retention domain (Fig 7A). This was due to a physical loss of virion secretion as opposed to changes in infectivity, because qPCR of viral genomes from the supernatant demonstrated a comparable loss in genome numbers as PFU (Fig 7B). Purification of virions demonstrated that, as in earlier data (Fig 3H), loss of gpUL141 led to increases in levels of all gpUL141-interacting proteins, with loss of just the ER retention domain resulting in increased levels of some gH-complex containing proteins, with gO in particular restored (Fig 7C). Thus, the alteration in growth properties associated with gpUL141 expression arises from the presence of the ER retention domain, which also modulates some virion glycoprotein levels in the virion.

We have previously found that modulating the expression levels of gH-containing complexes alters the sensitivity of HCMV to neutralising antibodies during spread within a monolayer[15]. To determine whether the changes seen here had a similar impact, we infected cells at low MOI with

GFP-expressing HCMV strains that either contained or lacked UL141, and measured dissemination over time in the presence of cytotect, a pooled polyclonal preparation of antibodies from HCMV seropositive individuals and selected for high neutralising activity. Whereas wildtype virus was completely resistant to neutralising antibodies, virus lacking UL141 was susceptible (Fig 7D).

Therefore, gpUL141 contains an ER retention domain which is not required for its NK-evasion properties, but acts to restrict cell-surface expression of gB and all gH-containing glycoprotein complexes, while also affecting virion envelope composition. This reduces virus dissemination, but renders it more resistant to both neutralising antibodies and ADCC. Thus, UL141 acts as an evasin of both innate (NK) and adaptive (humoral) immunity.

Discussion

Even though HCMV has the largest genome of any human virus, capsid packaging requirements still limit genome size[54], necessitating to the evolution of polyfunctional proteins. gpUL141 was previously recognised to promote virus survival through three distinct mechanisms (targeting CD155[14], CD112[13], all four TRAIL receptors[12]). As cell and virion surface proteins, there are multiple examples of viral entry glycoproteins being 'co-opted' to also act as immune evasins[55]. However, although gpUL141 is found in the virion in complex with nearly all HCMV entry glycoprotein complexes, our data argues that rather than acting in entry, gpUL141 acts to modulate the levels of other glycoproteins in order to control syncytia formation and avoid both neutralising and non-neutralising antibody-mediated control. Soluble gpUL141 can bind to CD155 on the cell surface (unpublished), implying that virion-presented gpUL141 could act in receptor-mediated viral entry. However, given that the presence of gpUL141 results in reduced virus dissemination and lower cell-free titres in epithelial and endothelial cells *in vitro*, any such functions do not seem to be proviral. Furthermore, the ability of gpUL141 to restrict growth was lost when the ER retention domain was removed, implying that this phenotype arises from influences on glycoprotein trafficking rather than receptor binding.

As a large and complex virus with a broad tropism, HCMV encodes over 10 different envelope glycoproteins that form the core receptor binding and envelope fusion functions[56]. gB transits via the plasma membrane before being internalised to be delivered to the viral assembly complex for virion incorporation[57], and presumably the same is true for other glycoproteins. All are therefore potential targets for humoral immunity on the infected cell surface. Through targeting two viral proteins (gH and gB) that are common to nearly all of these complexes, gpUL141 provides an elegant solution to this problem. Both knock-in (RAd) and knock-out (HCMV; both whole protein and ER-RD) support a model in which gpUL141 inhibits plasma-membrane transport and subsequent virion incorporation of the majority of HCMV entry glycoproteins. We have previously shown that the humoral ADCC response during natural infection is highly polyclonal, targeting numerous proteins from the early phase of the viral lifecycle onwards[58,59]. Using Merlin, ADCC activity peaked prior to the expression of entry glycoproteins. This could be in part due to UL141 limiting glycoprotein levels, however it is also possible that UL141-mediated intracellular retention is more important to limit the generation of ADCC-antibodies against entry glycoproteins during infection. Dissecting this will require isolating and mapping monoclonal antibodies that target gB and Trimer/Pentamer/UL116 that are ADCC-capable, as we have previously for gpUL141[60]. However, given the large number of antigens that gpUL141 influences, even small alterations in cell-surface levels have the potential to produce significant effects.

Although complete loss of gpUL141 resulted in robust effects on plasma membrane and virion envelope composition, the impact of removing just the ER-RD was more varied. Modulation of plasma membrane levels were either partially or entirely dependent on the ER-RD, depending on the assay and protein being tested. In the virion envelope loss of the ER-RD only partially phenocopied complete loss of gpUL141. This likely reflects the presence of multiple different competing signals within the C-terminal intracellular domain of gpUL141, all of which were lost by complete truncation. UL141 has an ER retention dilysine motif in it's C-terminus and also a YxxΦ motif for endosomal retrieval from the plasma membrane[61]. Trafficking through the ER can also depend on interactions between C-terminal and membrane domains[62]. Thus, gpUL141 may both limit ER-exit of glycoprotein complexes while also promoting re-internalisation into the VAC of those that do traffic to the cell surface. Loss of both motifs may influence multiple processes, with the final outcome also depending on the motifs found in component proteins of the different complexes – for example gB has its own retrieval motif[57]. Assessing this will require more in-depth analysis and targeted mutagenesis of the gpUL141 cytoplasmic tail.

Despite the partial effects seen biochemically following ER-RD deletion, effects on virus growth were almost entirely recovered, with the ΔER-RD virus producing higher cell-free titres. This may indicate a threshold effect, in which levels are restored 'enough' to improve virion infectivity – in particular gO, which is required for cell-free infectivity, was upregulated in this virus. These assays imply that for HCMV, reducing envelope glycoprotein levels in the virion may have an impact on virus infectivity, but this is a price worth paying if it also results in lower cell-surface antigenic targets for ADCC, resistance to neutralising antibodies, and lower syncytia formation.

The levels of multiple envelope glycoprotein complexes are notably different in Merlin compared to passaged HCMV strains. As a ratio, Merlin has higher levels of pentamer and lower levels of trimer[63], and also expresses gpRL13[8]. At least some of these differences arise from *in vitro* acquired mutations in passaged strains[8,30], whether they can also arise from genuine strain-specific effects remains to be determined. Nevertheless, they result in Merlin disseminating via a form of cell-cell spread that is exceptionally resistant to neutralising antibodies[8,15]. Subsequent studies have shown that although these differences explain some of the antibody-resistance of Merlin, they are not the only factor[64]. gpUL141 provides an explanation for these observations[37]. There may also be interplay between gpUL141 and other viral proteins that modulate entry glycoprotein trafficking. UL148 leads to reduction of pentamer levels in the virion in favour of trimer[65] by preventing gO degradation[36], while gpUL116 acts as a chaperone for gH to get to the cell surface[45,46] and trimer incorporation into the virion[30]. Further work will be needed to investigate these impacts in the presence of UL141.

Our work also explains the long-standing observation that the UL140-145 genome region is frequently lost when clinical HCMV strains are passaged *in vitro*[31,66]. When clinical viruses underwent extensive *in vitro* passage, mutations adjacent-to or involving UL141 were seen in 2/3 strains, in fibroblast, epithelial, and endothelial cells[15]. When Merlin was passaged in epithelial cells, mutations in UL141 were invariably selected[67], and laboratory strains frequently contain mutations in UL141, including TB40[14,68], VR1814 and the derived FIX-BAC[14], and all AD169 variants including those with less extensive mutations such as AD169varUC[56]. UL141 is clearly detrimental to virus release and dissemination in epithelial and endothelial cells, however these studies imply that it may also be detrimental in fibroblasts. No growth phenotype was associated with UL141 in Merlin in fibroblasts, possibly because the effects on virion incorporation were weaker than in epithelial cells. Nevertheless, it is clear that gpUL141 can reduce glycoprotein incorporation into the virion in fibroblasts. gO is hypervariable[69,70] and variants influence other

glycoproteins as well as virus growth in diverse ways[31,66,71,72]. Therefore, different phenotypes may be observed when viruses encode other gO genotypes.

The actions of gpUL141 imply that it is beneficial to HCMV not to form syncytia. The role of syncytia *in vivo* remains unclear, however HCMV strains that lack UL141 can form syncytia in a range of cell types *in vitro* including labial & lung fibroblasts[60], cerebral organoids[63], Forebrain neurons[73], and Renal Proximal Tubule Epithelial Cells[74]. It is clear from these studies that different cell types vary in their ability to support HCMV-induced syncytia, and that different variants of other viral proteins such as gB can dramatically influence this[58,59]. UL141 may modulate the extent to which these differences alter cell fusion, but are unlikely to completely prevent it since we still saw small syncytia (2 nuclei) during infection of ARPE19 cells even when UL141 was expressed.

Overall, gpUL141 represents a novel viral strategy for immune evasion encoded by HCMV, which impacts numerous aspects of the lifecycle that are relevant to therapeutic and vaccine design. It is therefore important that strains intact for gpUL141 are tested during preclinical development.

Methods

Cell Culture

Human foetal foreskin fibroblasts (HFFFs) immortalised with human telomerase reverse transcriptase (HF-TERTs)[75], HF-TERT-immortalized HFFFs expressing Coxsackie adenovirus receptor (HF-CAR)[15], and retinal pigment epethilial-1 (RPE-1) cells were maintained under standard conditions in DMEM (Sigma) supplemented with 10% heat-inactivated fetal bovine serum (Sigma). Human umbilical vein endothelial cells (HUVEC) were maintained under standard conditions in Endothelial Cell Growth Medium (Basal medium plus individual supplements; PromoCell).

Viruses and Infections

HCMV variants were recovered from an infectious bacterial artificial chromosome (BAC) clone of strain Merlin. This encodes the complete strain Merlin genome, which was repaired to match the sequence of the original clinical material[8]. Mutations are rapidly selected in the genes encoding RL13 and UL128L upon passage *in vitro*, therefore the promoters for these genes have been rendered responsive to the tetracycline repressor (TetR). In cells expressing tetR, expression is restricted, allowing recovery of genetically intact virus[42]. This virus loses tropism for cell types other than fibroblasts due to repression of UL128L, but can readily infect fibroblasts. If these fibroblasts lack tetR then UL128L is expressed, and virus can be transferred to other cell types (e.g. endothelial and epithelial cells) by co-culture. Deletion of the UL141 ER retention domain was carried out by en-passant mutagenesis[76] with primers 5'-ACACACTGCATTTTTTAACATCTTATTTTTTTATTTTATGCGTGTTCTCAACAGCACTGCAGGTAACACATAGGGATAACAGGGTAATCGATTT-3' and 5'-TTTTGGAGTATTTTCACCGTATGTTTCCTATGCTACCTGTGTTACCTGCAGTGCTGTTGAGAACACGCATAAAATAAGCCAGTGTTACAACCAATTAACC-3'. A V5 epitope tag was added to the C-terminus of UL141 by recombineering as previously described[8], using primers 5'-AGGGGACGACGAGGCGGTGAGGGCTATCGACGCCTACCGACTTACGATAGTTACCCCGGTGTTAAAAAGATGAAGAGGCCTGTGACGGAAGATCACTTCG-3' and 5'-GCATATTTTAATCACACTATTCACATTTCACACACTGCATTTTTTAACATCTTATTTTTTTATTTTATGCGTGTTCTCACTGAGGTTCTTATGGCTCTTG-3' to insert the SacB cassette and primers 5'-GACGCCTACCGACTTACGATAGTTACCCCGGTGTTAAAAAGATGAAGAGGGGCTCCGGGGGGTCGGGTGGAAGTGGCGGTAAGCCAATCCCTAACCCGCT-3' and 5'-ACACACTGCATTTTTTAACATCTTATTTTTTTATTTTATGCGTGTTCTCACGTAGAATCAAGACCTAGGAGCGGGTTAGGGATTGGCTTACCGCCACTTC-3' to replace the cassette with a V5 epitope tag. A HA tag was added to the C-terminus of UL116 by en-passant mutagenesis using primers 5'-ACCTGAGTGCCAACTTTTGGCGCCAACTGGCTCCTTACCGTCACACTCTCATCGTGCCGCAGACTAGCGCTTACCCCTACGACGTGCCCGACTACGCCTG-3' and 5'-CAACACCACAGCAGTATCACCGGTCCAGGTGAGAAAGAGAAGCCGCAATCCGGGCGGCGGCACATCAGGCGTAGTCGGGCACGTCGTAGGGGTAAGCGCT-3'. Replication deficient Adenovirus vectors were constructed in the AdZ system as previously described[77]. All modifications were verified by sanger sequencing of the modified site, and all viruses underwent whole genome sequencing following recovery from the BAC[42].

Infectious HCMV was recovered by transfecting HF-Tet cells with an Amaxa Nucleofector, the basic fibroblast kit, and program T-16. Virus was harvested from the supernatant when 100% CPE was achieved, then cells remove by low speed centrifugation (420 x*g*, 3 min), before virus was pelleted by high speed centrifugation (29,500 x*g*, 2h). Virus was resuspended in DMEM containing

10% FCS, aliquoted, and stored at -80°C. Cell-free titres were determined using an IE1 micro plaque assay. Briefly, HF-Terts were seeded in 96-well plates 18 h prior to use. Virus supernatants were 10-fold serially diluted in DMEM-FBS and added to cells. At 24 h p.i. media was removed and cells fixed in ice cold 50:50 Acetone/Methanol for 15 min. Cells were washed once in PBS and primary antibody added at 1:1000 in PBS for 30 min at 37°C. Cells were washed once in PBS and secondary antibody added at 1:500 in PBS for 30 min at 37°C, followed by a final wash in PBS. Infected cells were counted using an Incucyte® (see below).

For proteomics and biochemical analysis cell-free virus was harvested from the supernatant, cell debris removed by low-speed centrifugation (420 xg, 3 min), then samples concentrated either by dialysis (Viva flow 50R, Sartorius, 1MDa cut-off) or by pelleting through a 20% sorbitol cushion (82,700 xg, 1 h). Intact virions were then separated from cellular debris, dense bodies, and non-infectious particles by positive density/negative viscosity gradient centrifugation, as previously described[78].

Unless otherwise stated HCMV infection of HF-Terts was at MOI=5 for 72 h. To infect RPE-1 or HUVEC cells, HF-Terts infected for 72h were co-cultured with target cells at ratios of 0.03:1, 1:2, or 4:1 HF-Tert:RPE-1/HUVEC for virus dissemination and syncytia analysis, growth kinetics, or PNGase F assays, respectively. For dissemination inhibition assays in HUVEC cells, Cytotect® was added to cells at 3 days post co-culture in a 10-fold serial dilution starting at 5000 µg/mL. HF-CARs were infected with RAd at MOIs stated, for 48 h.

Proteomics

For analysis of virions by MS, cells were passaged for two weeks in SILAC-DMEM containing arginine and lysine in either their normal, medium (13C6), or heavy (13C6-15N4, 13C6 15N2 respectively) forms respectively, before being infected and virus harvested and purified as above. Following purification samples were lysed in LDS sample buffer and run 1.5cm into a Bis-Tris Midi Gel (Thermo), before lanes were excised with a clean scalpel and cut into 6 equally sized bands. Samples were reduced, alkylated and digested in-gel using trypsin. Digested peptides were eluted with MeCN/water and 5% FA washes. Peptides were pooled in 0.5ml tubes (Protein LoBind, Eppendorf) and dried almost to completion. Samples were re-suspended in 15 µl solvent (3% MeCN, 0.1% TFA) with 7µl analysed by LC-MSMS using a Thermo Q Exactive mass spectrometer (Thermo Fischer Scientific) equipped with an EASYspray source and coupled to an RSLC3000 nano UPLC (Thermo Fischer Scientific). Peptides were fractionated using a 50cm C18 PepMap EASYspray column maintained at 35°C with a solvent flow rate of 250nl/min. A gradient was formed using solvent A (0.1% formic acid) and solvent B (80% acetonitrile, 0.1% formic acid) rising from 3% to 40% solvent B by 90 min followed by a 4 min wash at 95% solvent B. MS spectra were acquired at 70,000 resolution between m/z 400 and 1650 with MSMS spectra acquired at 17,500 fwhm following HCD activation. Data was processed in Maxquant 2.4.8.0 with carbamidomethyl (C) set as a fixed modification and oxidation (M) and acetyl (protein N-terminus) set as variable modifications. Data was searched against a Uniprot Homo Sapien database (downloaded 27/05/14) a curated database of canonical HCMV proteins and a database of common contaminants.

Separation of Subpopulations Following Co-culture

Where it was necessary to separate cell types following virus transfer by co-culture (e.g. for CD107a assays), a previously established magnetic-activated cell sorting (MACS) separation protocol was used[79]. In brief, HFFF expressing His-tagged mCherry protein on their cell surface were infected with HCMV for 72h, then co-cultured with target cells. Twenty-four hours post co-

culture cell monolayers were washed and detached, stained with anti-His antibody (Antibody and Reagents Table) followed by anti-mouse-IgG magnetic beads (Miltenyi Biotec), and separated by MACS (Miltenyi Biotec). Newly infected RPE-1 or HUVEC cells were maintained for a further 48 h prior to CD107a assay.

Immunoprecipitation

Cells or viruses were lysed in IP Lysis Buffer (Pierce) for 10 min in the presence of protease inhibitors (Sigma), then nuclei removed by centrifugation. Lysates were incubated with anti-V5 or anti-HA agarose beads (Abcam) overnight, before being washed 3 times in lysis buffer and proteins eluted by boiling for 10 min in 4X LDS sample buffer (Thermo Fisher).

PNGaseF and EndoH digestion

Samples were digested according to manufacturers instructions (NEB). In brief, samples were lysed in denaturing buffer then the appropriate reaction buffer added, and incubated overnight at 37°C in the presence of enzyme. Samples without enzyme added served as controls. The next day LDS sample buffer was added and samples boiled for 10 min before being analysed by SDS-PAGE and western blot.

Western blot

Samples were lysed in 4X LDS sample buffer (Thermo Fisher) then boiled for 10 min before being loaded onto Bis-Tris Midi gels (Thermo Fisher) and run for 1 h at 20V. Following separation samples were transferred onto PVDF (Amersham) by semi-dry blotting, then blocked in 5% Milk/PBST (blocking buffer) for 1 h. Primary antibodies were added in blocking buffer for 1 h at room temperature or overnight at 4°C, washed 3x in PBST, then secondary HRP-conjugated antibodies added in blocking buffer for 1 h. After washing 3x in PBST membranes were incubated with supersignal west pico (Thermo Fisher) and imaged on a Syngene XX6 geldoc.

CD107a Assay

PBMCs were isolated from healthy donors and rested overnight in RPMI supplemented with 10% FCS, and L-glutamine (2 mM). Target cells were harvested using TrypLE Express (Thermo Fisher), then mixed with PBMC at an effector:target ratio of 10:1 in the presence of golgistop (0.7 µl/ml, BD Biosciences) anti-CD107a–FITC (clone H4A3, BioLegend), and relevant anti-HCMV antibodies. Cells were incubated for 5 h at 37°C, washed in cold PBS, and stained with live/dead Fixable Aqua (Thermo Fisher), anti-CD3–PECy7 (clone UCHT1, BioLegend), anti-CD56–BV605 (clone 5.1H11, BioLegend), anti-CD57–APC (clone HNK-1, BioLegend). Data were acquired using an Attune NxT Flow Cytometer (Thermo Fisher) and analysed with FlowJo software version 10 (FlowJo LLC).

Flow Cytometry

Cells were washed in PBS, dissociated with TrypLE Express (Thermo Fisher) and stained with primary antibody (Antibody and Reagents Table) for 30 min at 4°C. Cells were washed in PBS and incubated with the secondary antibody for 30 min at 4°C before being washed and fixed with 4% paraformaldehyde (PFA). All data was acquired using an Attune Nxt Flow Cytometer (Thermo Fisher), and analysed using FlowJo Software version 10 (FlowJo LLC).

qPCR

Viral DNA was extracted from DNase I treated (RQ1 RNase-free DNase; Promega) supernatants with the QIAamp MinElute Virus Spin Kit (Qiagen) as per manufacturers' instructions. Quantitative PCR reactions were performed in a Applied Biosystems Quant Studio 3 Thermal

Cycler (Thermo Fisher Scientific). Reactions were set up using FastGene 2x IC Green qPCR Universal Mix (Nippon Genetics; Geneflow), 0.4 µM of forward and reverse primers, and 100 ng of cDNA in a final volume of 20 µL. The gB forward primer was 5'-CTGCGTGATATGAACGTGAAGG-3' and the reverse primer was 5'-ACTGCACGTACGAGCTGTTGG-3'. Amplification was performed using the Comparative cT with Melt programme (2 min at 50°C, 10 min at 95°C, followed by 40 cycles of 15 sec at 95°C and 1 min at 60°C. Melt curve: 15 sec at 95°C, 1 min at 60°C and 15 sec at 95°C). Water-only negative controls and a serial dilution of a positive control standard (plasmid containing gB) were included in each run. CMV genome equivalents were calculated from the Ct values generated in The Standard Curve App (Thermo Fisher Scientific Connect Data Analysis Apps).

Incucyte®

Virus dissemination assays and virus titrations were measured on an Incucyte® SX5 Live Cell Analysis System, scanning the whole well with a 4X lens, with both brightfield and green image channels. Wells were scanned every 24 h for 10 days for dissemination and neutralisation assays, or one-off scans for titrations. Incucyte® Basic Analysis Software was used to measure the Total Integrated Intensity (GCU x μ^2/well) for time course analyses, or Count (per well) for titrations.

Syncytia Imaging and Analysis

Images were taken from 10 randomly selected fields of view at 20X magnification on a Zeiss Apotome 2 microscope. Syncytia were determined by the presence of two or more nuclei observable within a single cell membrane. Cell area was measured using Zeiss Zen Lite v3.10 software and nuclei counted manually. The average area of fluorescence within syncytia was expressed as a percentage of the total fluorescent cell area.

Structure prediction

The structures of gH (UniProt Q6SW67 residues 25–719) in complex with gpUL141 (UniProt Q6RJQ3 residues 37–278) and UL116 (UniProt Q6SW34 residues 25–313), or of a trimer of gB (UniProt F5HB53 residues 25–751) in complex were predicted using AlphaFold3[47]. For all, predicted signal sequences and transmembrane regions were excluded from the sequence used for structure prediction. Structures were superposed and molecular images were generated using PyMOL (Schrödinger).

Data availability

Atomic coordinates and per-residue quality statistics for the AlphaFold3 models have been deposited in the University of Cambridge Apollo repository (DOI:). Raw proteomics files are available at PRiDE (DOI:).

Statistics

All statistical analyses were carried out in GraphPad Prism v10.4.0. All assays were carried out in a minimum of technical triplicate, and repeated at least 3 times. Statistical tests carried out for each assay are noted in figure legends.

Antibody and Reagents Table

Reagent	Source	Identifier

Primary antibodies for flow cytometry		
Mouse anti-CD155 (clone D171)	Invitrogen	MA5-13493
Mouse anti-CD112 (clone b-c12)	Santa Cruz	sc-65333
Mouse anti-TRAIL-R2 (human; clone HS201)	AdipoGen Life Sciences	AG-20B-0023
Mouse-anti CMV gH	BioRad	2470-5437
Mouse anti-gB (SM5-MsFC)	In-house	
Primary antibodies for immunoblotting		
Mouse anti-CMV gB (clone 2F12)	Abcam	ab6499
Mouse anti-CMV (IE1)	Merck	MAB810R
Mouse anti-gpUL141 (clones M550.2 and M550.3)	In house[14]	
Mouse anti-MCP (clone 28-4)	A gift from William Britt, University of Alabama, USA.	
Rabbit anti-gH	A gift from Brent Ryckman, University of Montana[66]	
Rabbit anti-gL	A gift from Brent Ryckman, University of Montana[66]	
Mouse anti-gO	A gift from Stipan Jonjic[80]	
Mouse anti-gpUL116	Gift from Marcello Merona, University at Naples, Italy[36]	
Mouse anti-gpUL128	A gift from Giuseppe Gerna[81]	
Mouse anti-human HLA-A/B/C (clone W6/32)	BioLegend	311402
Mouse anti-V5 tag	BioRad	MCA1360
Rabbit anti-V5	Abcam	ab9116
Anti-HA Tag (clone 11A3A05)	BioLegend	660002
Rabbit Anti-Actin	Sigma	A2066
Antibodies for CD107a assay		
Mouse FITC anti-human CD107a	BioLegend	328606
Mouse PE/Cy7 anti-human CD3	BioLegend	300420

Mouse APC anti-human CD57	BioLegend	359610
Mouse BV605 anti-human CD56	BioLegend	362538
Primary antibody for titration		
Mouse anti-CMV (IE1)	Merck	MAB810R
Secondary antibodies		
Goat anti-mouse HRP	BioRad	170-6516
Goat anti-rabbit HRP	BioRad	170-6515
Goat anti-mouse Alexa Fluor 488	Invitrogen	A11017
Goat anti-mouse Alexa Fluor 647	Invitrogen	A21235
Goat anti-rabbit Alexa Fluor 647	Invitrogen	A21246
Antibodies and Reagents for MACS Separation		
Mouse anti-His (clone His.H8)	Thermo Fisher	MA1-21315
MACS anti-IgG MicroBeads	Miltenyi Biotec	130-048-401
MACS LS Columns	Miltenyi Biotec	130-042-401
MACS Separation Buffer	Miltenyi Biotec	130-091-221
MACS Pre-Separation Filters (70μM)	Miltenyi Biotec	130-095-823
Additional Reagents		
Aqua live/dead	Thermo Fisher	L34966
GolgiStop	BD Biosciences	554724
PNGase F	NEB	P0704
Endo H	NEB	P0702
Agarose anti-V5 tag	Abcam	ab1229
Agarose anti-HA tag	Abcam	ab214758
FastGene 2x IC Green qPCR Universal Mix	Geneflow	P8-0058

1. Dunn, W., Chou, C., Li, H., Hai, R., Patterson, D., Stolc, V., Zhu, H., and Liu, F. (2003). Functional profiling of a human cytomegalovirus genome. Proceedings of the National Academy of Sciences of the United States of America *100*, 14223-14228. 10.1073/pnas.2334032100.

2. Yu, D., Silva, M.C., and Shenk, T. (2003). Functional map of human cytomegalovirus AD169 defined by global mutational analysis. Proceedings of the National Academy of Sciences of the United States of America *100*, 12396-12401. 10.1073/pnas.1635160100.
3. Patel, M., Vlahava, V.M., Forbes, S.K., Fielding, C.A., Stanton, R.J., and Wang, E.C.Y. (2018). HCMV-Encoded NK Modulators: Lessons From in vitro and in vivo Genetic Variation. Frontiers in immunology *9*, 2214. 10.3389/fimmu.2018.02214.
4. Wilkinson, G.W., Tomasec, P., Stanton, R.J., Armstrong, M., Prod'homme, V., Aicheler, R., McSharry, B.P., Rickards, C.R., Cochrane, D., Llewellyn-Lacey, S., et al. (2008). Modulation of natural killer cells by human cytomegalovirus. Journal of clinical virology : the official publication of the Pan American Society for Clinical Virology *41*, 206-212. 10.1016/j.jcv.2007.10.027.
5. Jackson, S.E., Mason, G.M., and Wills, M.R. (2011). Human cytomegalovirus immunity and immune evasion. Virus research *157*, 151-160. 10.1016/j.virusres.2010.10.031.
6. Dargan, D.J., Douglas, E., Cunningham, C., Jamieson, F., Stanton, R.J., Baluchova, K., McSharry, B.P., Tomasec, P., Emery, V.C., Percivalle, E., et al. (2010). Sequential mutations associated with adaptation of human cytomegalovirus to growth in cell culture. The Journal of general virology *91*, 1535-1546. 10.1099/vir.0.018994-0.
7. Wilkinson, G.W., Davison, A.J., Tomasec, P., Fielding, C.A., Aicheler, R., Murrell, I., Seirafian, S., Wang, E.C., Weekes, M., Lehner, P.J., et al. (2015). Human cytomegalovirus: taking the strain. Medical microbiology and immunology *204*, 273-284. 10.1007/s00430-015-0411-4.
8. Stanton, R.J., Baluchova, K., Dargan, D.J., Cunningham, C., Sheehy, O., Seirafian, S., McSharry, B.P., Neale, M.L., Davies, J.A., Tomasec, P., et al. (2010). Reconstruction of the complete human cytomegalovirus genome in a BAC reveals RL13 to be a potent inhibitor of replication. The Journal of clinical investigation *120*, 3191-3208. 10.1172/JCI42955.
9. Rubina, A., Patel, M., Nightingale, K., Potts, M., Fielding, C.A., Kollnberger, S., Lau, B., Ladell, K., Miners, K.L., Nichols, J., et al. (2023). ADAM17 targeting by human cytomegalovirus remodels the cell surface proteome to simultaneously regulate multiple immune pathways. Proceedings of the National Academy of Sciences of the United States of America *120*, e2303155120. 10.1073/pnas.2303155120.
10. Vlahava, V.M., Murrell, I., Zhuang, L., Aicheler, R.J., Lim, E., Miners, K.L., Ladell, K., Suarez, N.M., Price, D.A., Davison, A.J., et al. (2021). Monoclonal antibodies targeting nonstructural viral antigens can activate ADCC against human cytomegalovirus. The Journal of clinical investigation *131*. 10.1172/JCI139296.
11. Stanton, R.J., Prod'homme, V., Purbhoo, M.A., Moore, M., Aicheler, R.J., Heinzmann, M., Bailer, S.M., Haas, J., Antrobus, R., Weekes, M.P., et al. (2014). HCMV pUL135 remodels the actin cytoskeleton to impair immune recognition of infected cells. Cell Host Microbe *16*, 201-214. 10.1016/j.chom.2014.07.005.
12. Smith, W., Tomasec, P., Aicheler, R., Loewendorf, A., Nemcovicova, I., Wang, E.C., Stanton, R.J., Macauley, M., Norris, P., Willen, L., et al. (2013). Human cytomegalovirus glycoprotein UL141 targets the TRAIL death receptors to thwart host innate antiviral defenses. Cell Host Microbe *13*, 324-335. 10.1016/j.chom.2013.02.003.
13. Prod'homme, V., Sugrue, D.M., Stanton, R.J., Nomoto, A., Davies, J., Rickards, C.R., Cochrane, D., Moore, M., Wilkinson, G.W.G., and Tomasec, P. (2010). Human cytomegalovirus UL141 promotes efficient downregulation of the natural killer cell activating ligand CD112. The Journal of general virology *91*, 2034-2039. 10.1099/vir.0.021931-0.
14. Tomasec, P., Wang, E.C., Davison, A.J., Vojtesek, B., Armstrong, M., Griffin, C., McSharry, B.P., Morris, R.J., Llewellyn-Lacey, S., Rickards, C., et al. (2005). Downregulation of natural killer cell-activating ligand CD155 by human cytomegalovirus UL141. Nature immunology *6*, 181-188. 10.1038/ni1156.

15. Murrell, I., Bedford, C., Ladell, K., Miners, K.L., Price, D.A., Tomasec, P., Wilkinson, G.W.G., and Stanton, R.J. (2017). The pentameric complex drives immunologically covert cell-cell transmission of wild-type human cytomegalovirus. Proceedings of the National Academy of Sciences of the United States of America *114*, 6104-6109. 10.1073/pnas.1704809114.
16. Weekes, M.P., Tomasec, P., Huttlin, E.L., Fielding, C.A., Nusinow, D., Stanton, R.J., Wang, E.C.Y., Aicheler, R., Murrell, I., Wilkinson, G.W.G., et al. (2014). Quantitative temporal viromics: an approach to investigate host-pathogen interaction. Cell *157*, 1460-1472. 10.1016/j.cell.2014.04.028.
17. Hsu, J.L., van den Boomen, D.J., Tomasec, P., Weekes, M.P., Antrobus, R., Stanton, R.J., Ruckova, E., Sugrue, D., Wilkie, G.S., Davison, A.J., et al. (2015). Plasma membrane profiling defines an expanded class of cell surface proteins selectively targeted for degradation by HCMV US2 in cooperation with UL141. PLoS pathogens *11*, e1004811. 10.1371/journal.ppat.1004811.
18. Karniely, S., Weekes, M.P., Antrobus, R., Rorbach, J., van Haute, L., Umrania, Y., Smith, D.L., Stanton, R.J., Minczuk, M., Lehner, P.J., and Sinclair, J.H. (2016). Human Cytomegalovirus Infection Upregulates the Mitochondrial Transcription and Translation Machineries. MBio *7*, e00029. 10.1128/mBio.00029-16.
19. Fielding, C.A., Weekes, M.P., Nobre, L.V., Ruckova, E., Wilkie, G.S., Paulo, J.A., Chang, C., Suarez, N.M., Davies, J.A., Antrobus, R., et al. (2017). Control of immune ligands by members of a cytomegalovirus gene expansion suppresses natural killer cell activation. Elife *6*. 10.7554/eLife.22206.
20. Nightingale, K., Lin, K.M., Ravenhill, B.J., Davies, C., Nobre, L., Fielding, C.A., Ruckova, E., Fletcher-Etherington, A., Soday, L., Nichols, H., et al. (2018). High-Definition Analysis of Host Protein Stability during Human Cytomegalovirus Infection Reveals Antiviral Factors and Viral Evasion Mechanisms. Cell Host Microbe *24*, 447-460 e411. 10.1016/j.chom.2018.07.011.
21. Wang, E.C.Y., Pjechova, M., Nightingale, K., Vlahava, V.M., Patel, M., Ruckova, E., Forbes, S.K., Nobre, L., Antrobus, R., Roberts, D., et al. (2018). Suppression of costimulation by human cytomegalovirus promotes evasion of cellular immune defenses. Proceedings of the National Academy of Sciences of the United States of America *115*, 4998-5003. 10.1073/pnas.1720950115.
22. Nobre, L.V., Nightingale, K., Ravenhill, B.J., Antrobus, R., Soday, L., Nichols, J., Davies, J.A., Seirafian, S., Wang, E.C., Davison, A.J., et al. (2019). Human cytomegalovirus interactome analysis identifies degradation hubs, domain associations and viral protein functions. Elife *8*. 10.7554/eLife.49894.
23. Fletcher-Etherington, A., Nobre, L., Nightingale, K., Antrobus, R., Nichols, J., Davison, A.J., Stanton, R.J., and Weekes, M.P. (2020). Human cytomegalovirus protein pUL36: A dual cell death pathway inhibitor. Proceedings of the National Academy of Sciences of the United States of America *117*, 18771-18779. 10.1073/pnas.2001887117.
24. Clement, M., Forbester, J.L., Marsden, M., Sabberwal, P., Sommerville, M.S., Wellington, D., Dimonte, S., Clare, S., Harcourt, K., Yin, Z., et al. (2022). IFITM3 restricts virus-induced inflammatory cytokine production by limiting Nogo-B mediated TLR responses. Nature communications *13*, 5294. 10.1038/s41467-022-32587-4.
25. Nightingale, K., Potts, M., Hunter, L.M., Fielding, C.A., Zerbe, C.M., Fletcher-Etherington, A., Nobre, L., Wang, E.C.Y., Strang, B.L., Houghton, J.W., et al. (2022). Human cytomegalovirus protein RL1 degrades the antiviral factor SLFN11 via recruitment of the CRL4 E3 ubiquitin ligase complex. Proceedings of the National Academy of Sciences of the United States of America *119*, e2108173119. 10.1073/pnas.2108173119.
26. Vlachava, V.M., Seirafian, S., Fielding, C.A., Kollnberger, S., Aicheler, R.J., Hughes, J., Baker, A., Weekes, M.P., Forbes, S., Wilkinson, G.W.G., et al. (2023). HCMV-secreted

glycoprotein gpUL4 inhibits TRAIL-mediated apoptosis and NK cell activation. Proceedings of the National Academy of Sciences of the United States of America *120*, e2309077120. 10.1073/pnas.2309077120.

27. Li, H., Fletcher-Etherington, A., Hunter, L.M., Keshri, S., Fielding, C.A., Nightingale, K., Ravenhill, B., Nobre, L., Potts, M., Antrobus, R., et al. (2024). Human cytomegalovirus degrades DMXL1 to inhibit autophagy, lysosomal acidification, and viral assembly. Cell Host Microbe. 10.1016/j.chom.2024.02.013.
28. Varnum, S.M., Streblow, D.N., Monroe, M.E., Smith, P., Auberry, K.J., Pasa-Tolic, L., Wang, D., Camp, D.G., 2nd, Rodland, K., Wiley, S., et al. (2004). Identification of proteins in human cytomegalovirus (HCMV) particles: the HCMV proteome. J Virol *78*, 10960-10966. 10.1128/JVI.78.20.10960-10966.2004.
29. Bogdanow, B., Gruska, I., Mühlberg, L., Protze, J., Hohensee, S., Vetter, B., Bosse, J.B., Lehmann, M., Sadeghi, M., Wiebusch, L., and Liu, F. (2023). Spatially resolved protein map of intact human cytomegalovirus virions. Nature Microbiology *8*, 1732-1747. 10.1038/s41564-023-01433-8.
30. Murrell, I., Tomasec, P., Wilkie, G.S., Dargan, D.J., Davison, A.J., and Stanton, R.J. (2013). Impact of sequence variation in the UL128 locus on production of human cytomegalovirus in fibroblast and epithelial cells. J Virol *87*, 10489-10500. 10.1128/JVI.01546-13.
31. Zhang, L., Zhou, M., Stanton, R., Kamil, J., and Ryckman, B.J. (2018). Expression Levels of Glycoprotein O (gO) Vary between Strains of Human Cytomegalovirus, Influencing the Assembly of gH/gL Complexes and Virion Infectivity. J Virol *92*. 10.1128/JVI.00606-18.
32. Vezzani, G., Pimazzoni, S., Ferranti, R., Calò, S., Monda, G., Amendola, D., Frigimelica, E., Maione, D., Cortese, M., and Merola, M. (2022). Human immunoglobulins are transported to HCMV viral envelope by viral Fc gamma receptors-dependent and independent mechanisms. Frontiers in microbiology *13*, 1106401. 10.3389/fmicb.2022.1106401.
33. Wang, D., and Shenk, T. (2005). Human cytomegalovirus virion protein complex required for epithelial and endothelial cell tropism. Proceedings of the National Academy of Sciences of the United States of America *102*, 18153-18158. 10.1073/pnas.0509201102.
34. Adler, B., Scrivano, L., Ruzcics, Z., Rupp, B., Sinzger, C., and Koszinowski, U. (2006). Role of human cytomegalovirus UL131A in cell type-specific virus entry and release. The Journal of general virology *87*, 2451-2460. 10.1099/vir.0.81921-0.
35. Krishna, B.A., Miller, W.E., and O'Connor, C.M. (2018). US28: HCMV's Swiss Army Knife. Viruses *10*. 10.3390/v10080445.
36. Calo, S., Cortese, M., Ciferri, C., Bruno, L., Gerrein, R., Benucci, B., Monda, G., Gentile, M., Kessler, T., Uematsu, Y., et al. (2016). The Human Cytomegalovirus UL116 Gene Encodes an Envelope Glycoprotein Forming a Complex with gH Independently from gL. J Virol *90*, 4926-4938. 10.1128/JVI.02517-15.
37. Li, G., Nguyen, C.C., Ryckman, B.J., Britt, W.J., and Kamil, J.P. (2015). A viral regulator of glycoprotein complexes contributes to human cytomegalovirus cell tropism. Proceedings of the National Academy of Sciences of the United States of America *112*, 4471-4476. 10.1073/pnas.1419875112.
38. Adair, R., Douglas, E.R., Maclean, J.B., Graham, S.Y., Aitken, J.D., Jamieson, F.E., and Dargan, D.J. (2002). The products of human cytomegalovirus genes UL23, UL24, UL43 and US22 are tegument components. The Journal of general virology *83*, 1315-1324. 10.1099/0022-1317-83-6-1315.
39. Reyda, S., Tenzer, S., Navarro, P., Gebauer, W., Saur, M., Krauter, S., Buscher, N., and Plachter, B. (2014). The tegument protein pp65 of human cytomegalovirus acts as an optional scaffold protein that optimizes protein uploading into viral particles. J Virol *88*, 9633-9646. 10.1128/JVI.01415-14.

40. Malouli, D., Nakayasu, E.S., Viswanathan, K., Camp, D.G., 2nd, Chang, W.L., Barry, P.A., Smith, R.D., and Fruh, K. (2012). Reevaluation of the coding potential and proteomic analysis of the BAC-derived rhesus cytomegalovirus strain 68-1. J Virol *86*, 8959-8973. 10.1128/JVI.01132-12.
41. Kattenhorn, L.M., Mills, R., Wagner, M., Lomsadze, A., Makeev, V., Borodovsky, M., Ploegh, H.L., and Kessler, B.M. (2004). Identification of proteins associated with murine cytomegalovirus virions. J Virol *78*, 11187-11197. 10.1128/JVI.78.20.11187-11197.2004.
42. Murrell, I., Wilkie, G.S., Davison, A.J., Statkute, E., Fielding, C.A., Tomasec, P., Wilkinson, G.W., and Stanton, R.J. (2016). Genetic Stability of Bacterial Artificial Chromosome-Derived Human Cytomegalovirus during Culture In Vitro. J Virol *90*, 3929-3943. 10.1128/JVI.02858-15.
43. Wu, Y., Prager, A., Boos, S., Resch, M., Brizic, I., Mach, M., Wildner, S., Scrivano, L., and Adler, B. (2017). Human cytomegalovirus glycoprotein complex gH/gL/gO uses PDGFR-alpha as a key for entry. PLoS pathogens *13*, e1006281. 10.1371/journal.ppat.1006281.
44. Kschonsak, M., Rouge, L., Arthur, C.P., Hoangdung, H., Patel, N., Kim, I., Johnson, M.C., Kraft, E., Rohou, A.L., Gill, A., et al. (2021). Structures of HCMV Trimer reveal the basis for receptor recognition and cell entry. Cell *184*, 1232-1244 e1216. 10.1016/j.cell.2021.01.036.
45. Vezzani, G., Amendola, D., Yu, D., Chandramouli, S., Frigimelica, E., Maione, D., and Merola, M. (2021). The Human Cytomegalovirus UL116 Glycoprotein Is a Chaperone to Control gH-Based Complexes Levels on Virions. Frontiers in microbiology *12*, 630121. 10.3389/fmicb.2021.630121.
46. Siddiquey, M.N.A., Schultz, E.P., Yu, Q., Amendola, D., Vezzani, G., Yu, D., Maione, D., Lanchy, J.M., Ryckman, B.J., Merola, M., and Kamil, J.P. (2021). The human cytomegalovirus protein UL116 interacts with the viral ER resident glycoprotein UL148 and promotes the incorporation of gH/gL complexes into virions. J Virol. 10.1128/JVI.02207-20.
47. Abramson, J., Adler, J., Dunger, J., Evans, R., Green, T., Pritzel, A., Ronneberger, O., Willmore, L., Ballard, A.J., Bambrick, J., et al. (2024). Accurate structure prediction of biomolecular interactions with AlphaFold 3. Nature *630*, 493-500. 10.1038/s41586-024-07487-w.
48. Nemcovicova, I., Benedict, C.A., and Zajonc, D.M. (2013). Structure of human cytomegalovirus UL141 binding to TRAIL-R2 reveals novel, non-canonical death receptor interactions. PLoS pathogens *9*, e1003224. 10.1371/journal.ppat.1003224.
49. Nemcovicova, I., and Zajonc, D.M. (2014). The structure of cytomegalovirus immune modulator UL141 highlights structural Ig-fold versatility for receptor binding. Acta crystallographica. Section D, Biological crystallography *70*, 851-862. 10.1107/S1399004713033750.
50. Ciferri, C., Chandramouli, S., Donnarumma, D., Nikitin, P.A., Cianfrocco, M.A., Gerrein, R., Feire, A.L., Barnett, S.W., Lilja, A.E., Rappuoli, R., et al. (2015). Structural and biochemical studies of HCMV gH/gL/gO and Pentamer reveal mutually exclusive cell entry complexes. Proceedings of the National Academy of Sciences of the United States of America *112*, 1767-1772. 10.1073/pnas.1424818112.
51. Weekes, M.P., Antrobus, R., Lill, J.R., Duncan, L.M., Hör, S., and Lehner, P.J. (2010). Comparative analysis of techniques to purify plasma membrane proteins. J Biomol Tech *21*, 108-115.
52. Vanarsdall, A.L., Ryckman, B.J., Chase, M.C., and Johnson, D.C. (2008). Human cytomegalovirus glycoproteins gB and gH/gL mediate epithelial cell-cell fusion when expressed either in cis or in trans. J Virol *82*, 11837-11850. 10.1128/JVI.01623-08.
53. Gerna, G., Percivalle, E., Perez, L., Lanzavecchia, A., and Lilleri, D. (2016). Monoclonal Antibodies to Different Components of the Human Cytomegalovirus (HCMV) Pentamer

gH/gL/pUL128L and Trimer gH/gL/gO as well as Antibodies Elicited during Primary HCMV Infection Prevent Epithelial Cell Syncytium Formation. J Virol *90*, 6216-6223. 10.1128/JVI.00121-16.

54. Yu, X., Jih, J., Jiang, J., and Zhou, Z.H. (2017). Atomic structure of the human cytomegalovirus capsid with its securing tegument layer of pp150. Science *356*. 10.1126/science.aam6892.
55. Cook, J.D., and Lee, J.E. (2013). The secret life of viral entry glycoproteins: moonlighting in immune evasion. PLoS pathogens *9*, e1003258. 10.1371/journal.ppat.1003258.
56. Bradley, A.J., Lurain, N.S., Ghazal, P., Trivedi, U., Cunningham, C., Baluchova, K., Gatherer, D., Wilkinson, G.W.G., Dargan, D.J., and Davison, A.J. (2009). High-throughput sequence analysis of variants of human cytomegalovirus strains Towne and AD169. The Journal of general virology *90*, 2375-2380. 10.1099/vir.0.013250-0.
57. Radsak, K., Eickmann, M., Mockenhaupt, T., Bogner, E., Kern, H., Eis-Hübinger, A., and Reschke, M. (1996). Retrieval of human cytomegalovirus glycoprotein B from the infected cell surface for virus envelopment. Archives of virology *141*, 557-572.
58. Tang, J., Frascaroli, G., Lebbink, R.J., Ostermann, E., and Brune, W. (2019). Human cytomegalovirus glycoprotein B variants affect viral entry, cell fusion, and genome stability. Proceedings of the National Academy of Sciences of the United States of America *116*, 18021-18030. 10.1073/pnas.1907447116.
59. Cimato, G., Zhou, X., Brune, W., and Frascaroli, G. (2024). Human cytomegalovirus glycoprotein variants governing viral tropism and syncytium formation in epithelial cells and macrophages. J Virol, e0029324. 10.1128/jvi.00293-24.
60. Aguiar, A., Galinato, M., Bradley Silva, M., Toth, B., McVoy, M.A., and Hertel, L. (2021). Human Cytomegalovirus Replication and Infection-Induced Syncytia Formation in Labial, Foreskin, and Fetal Lung Fibroblasts. Viruses *13*. 10.3390/v13122355.
61. Bonifacino, J.S., and Traub, L.M. (2003). Signals for Sorting of Transmembrane Proteins to Endosomes and Lysosomes*. Annual Review of Biochemistry *72*, 395-447. https://doi.org/10.1146/annurev.biochem.72.121801.161800.
62. Nilsson, T., and Warren, G. (1994). Retention and retrieval in the endoplasmic reticulum and the Golgi apparatus. Curr Opin Cell Biol *6*, 517-521. 10.1016/0955-0674(94)90070-1.
63. Egilmezer, E., Hamilton, S.T., Foster, C.S.P., Marschall, M., and Rawlinson, W.D. (2024). Human cytomegalovirus (CMV) dysregulates neurodevelopmental pathways in cerebral organoids. Commun Biol *7*, 340. 10.1038/s42003-024-05923-1.
64. Wu, H., Kropff, B., Mach, M., and Britt, W.J. (2020). Human Cytomegalovirus Envelope Protein gpUL132 Regulates Infectious Virus Production through Formation of the Viral Assembly Compartment. MBio *11*. 10.1128/mBio.02044-20.
65. Nguyen, C.C., Siddiquey, M.N.A., Zhang, H., Li, G., and Kamil, J.P. (2018). Human Cytomegalovirus Tropism Modulator UL148 Interacts with SEL1L, a Cellular Factor That Governs Endoplasmic Reticulum-Associated Degradation of the Viral Envelope Glycoprotein gO. J Virol *92*. 10.1128/JVI.00688-18.
66. Zhou, M., Yu, Q., Wechsler, A., and Ryckman, B.J. (2013). Comparative analysis of gO isoforms reveals that strains of human cytomegalovirus differ in the ratio of gH/gL/gO and gH/gL/UL128-131 in the virion envelope. J Virol *87*, 9680-9690. 10.1128/JVI.01167-13.
67. Schultz, E.P., Lanchy, J.M., Day, L.Z., Yu, Q., Peterson, C., Preece, J., and Ryckman, B.J. (2020). Specialization for Cell-Free or Cell-to-Cell Spread of BAC-Cloned Human Cytomegalovirus Strains Is Determined by Factors beyond the UL128-131 and RL13 Loci. J Virol *94*. 10.1128/JVI.00034-20.
68. Sinzger, C., Hahn, G., Digel, M., Katona, R., Sampaio, K.L., Messerle, M., Hengel, H., Koszinowski, U., Brune, W., and Adler, B. (2008). Cloning and sequencing of a highly productive, endotheliotropic virus strain derived from human cytomegalovirus TB40/E. The Journal of general virology *89*, 359-368. 10.1099/vir.0.83286-0.

69. Dolan, A., Cunningham, C., Hector, R.D., Hassan-Walker, A.F., Lee, L., Addison, C., Dargan, D.J., McGeoch, D.J., Gatherer, D., Emery, V.C., et al. (2004). Genetic content of wild-type human cytomegalovirus. The Journal of general virology *85*, 1301-1312. 10.1099/vir.0.79888-0.
70. Rasmussen, L., Geissler, A., Cowan, C., Chase, A., and Winters, M. (2002). The genes encoding the gCIII complex of human cytomegalovirus exist in highly diverse combinations in clinical isolates. J Virol *76*, 10841-10848. 10.1128/jvi.76.21.10841-10848.2002.
71. Day, L.Z., Stegmann, C., Schultz, E.P., Lanchy, J.M., Yu, Q., and Ryckman, B.J. (2020). Polymorphisms in Human Cytomegalovirus Glycoprotein O (gO) Exert Epistatic Influences on Cell-Free and Cell-to-Cell Spread and Antibody Neutralization on gH Epitopes. J Virol *94*. 10.1128/jvi.02051-19.
72. He, L., Taylor, S., Costa, C., Görzer, I., Kalser, J., Fu, T.M., Freed, D., Wang, D., Cui, X., Hertel, L., and McVoy, M.A. (2022). Polymorphic Forms of Human Cytomegalovirus Glycoprotein O Protect against Neutralization of Fibroblast Entry by Antibodies Targeting Epitopes Defined by Glycoproteins H and L. Viruses *14*. 10.3390/v14071508.
73. Adelman, J.W., Rosas-Rogers, S., Schumacher, M.L., Mokry, R.L., Terhune, S.S., and Ebert, A.D. (2023). Human cytomegalovirus induces significant structural and functional changes in terminally differentiated human cortical neurons. MBio, e0225123. 10.1128/mbio.02251-23.
74. Raviola, S., Griffante, G., Iannucci, A., Chandel, S., Lo Cigno, I., Lacarbonara, D., Caneparo, V., Pasquero, S., Favero, F., Corà, D., et al. (2024). Human cytomegalovirus infection triggers a paracrine senescence loop in renal epithelial cells. Communications Biology *7*, 292. 10.1038/s42003-024-05957-5.
75. McSharry, B.P., Jones, C.J., Skinner, J.W., Kipling, D., and Wilkinson, G.W.G. (2001). Human telomerase reverse transcriptase-immortalized MRC-5 and HCA2 human fibroblasts are fully permissive for human cytomegalovirus. The Journal of general virology *82*, 855-863. 10.1099/0022-1317-82-4-855.
76. Tischer, B.K., Smith, G.A., and Osterrieder, N. (2010). En passant mutagenesis: a two step markerless red recombination system. Methods in molecular biology *634*, 421-430. 10.1007/978-1-60761-652-8_30.
77. Stanton, R.J., McSharry, B.P., Armstrong, M., Tomasec, P., and Wilkinson, G.W. (2008). Re-engineering adenovirus vector systems to enable high-throughput analyses of gene function. Biotechniques *45*, 659-662, 664-658. 10.2144/000112993.
78. Irmiere, A., and Gibson, W. (1983). Isolation and characterization of a noninfectious virion-like particle released from cells infected with human strains of cytomegalovirus. Virology *130*, 118-133. 10.1016/0042-6822(83)90122-8.
79. Kerr-Jones, L.E., Soday, L., Hughes, N.C., Wang, X., Hunter, L.H., Antrobus, R., Miners, K.L., Ladell, K., Price, D.A., Fielding, C.A., et al. (2024). Highly Multiplexed Proteomic Analysis of HCMV-Infected Dendritic Cells Reveals Global Manipulation of Adaptive Immunity and Host Restriction of Viral Replication. bioRxiv, 2024.2004.2030.591855. 10.1101/2024.04.30.591855.
80. Laib Sampaio, K., Stegmann, C., Brizic, I., Adler, B., Stanton, R.J., and Sinzger, C. (2016). The contribution of pUL74 to growth of human cytomegalovirus is masked in the presence of RL13 and UL128 expression. The Journal of general virology *97*, 1917-1927. 10.1099/jgv.0.000475.
81. Gerna, G., Sarasini, A., Patrone, M., Percivalle, E., Fiorina, L., Campanini, G., Gallina, A., Baldanti, F., and Revello, M.G. (2008). Human cytomegalovirus serum neutralizing antibodies block virus infection of endothelial/epithelial cells, but not fibroblasts, early during primary infection. The Journal of general virology *89*, 853-865. 10.1099/vir.0.83523-0.

82. Kschonsak, M., Johnson, M.C., Schelling, R., Green, E.M., Rougé, L., Ho, H., Patel, N., Kilic, C., Kraft, E., Arthur, C.P., et al. (2022). Structural basis for HCMV Pentamer receptor recognition and antibody neutralization. Sci Adv *8*, eabm2536. 10.1126/sciadv.abm2536.
83. Chandramouli, S., Ciferri, C., Nikitin, P.A., Calo, S., Gerrein, R., Balabanis, K., Monroe, J., Hebner, C., Lilja, A.E., Settembre, E.C., and Carfi, A. (2015). Structure of HCMV glycoprotein B in the postfusion conformation bound to a neutralizing human antibody. Nature communications *6*, 8176. 10.1038/ncomms9176.

Figure 1

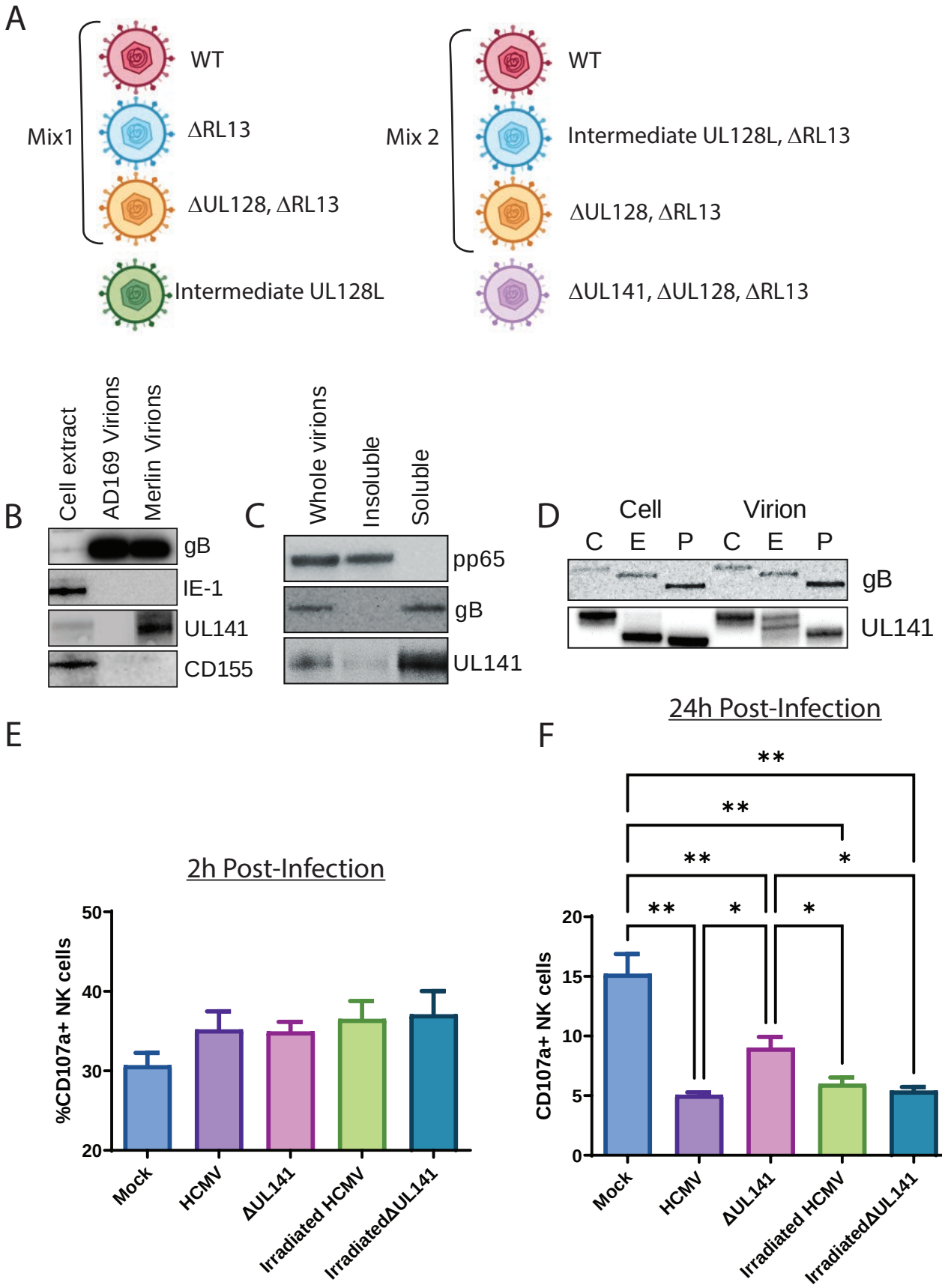
A
Mix1
WT
ΔRL13
ΔUL128, ΔRL13
Intermediate UL128L
Mix 2
WT
Intermediate UL128L, ΔRL13
ΔUL128, ΔRL13
ΔUL141, ΔUL128, ΔRL13
B
Cell extract
AD169 Virions
Merlin Virions
gB
IE-1
UL141
CD155
C
Whole virions
Insoluble
Soluble
pp65
gB
UL141
D
Cell
Virion
C E P C E P
gB
UL141
E
2h Post-Infection
%CD107a+ NK cells
50
40
30
20
Mock
HCMV
ΔUL141
Irradiated HCMV
IrradiatedΔUL141
F
24h Post-Infection
CD107a+ NK cells
20
15
10
5
0
**
**
**
*
**
*
*
Mock
HCMV
ΔUL141
Irradiated HCMV
IrradiatedΔUL141

Figure 2

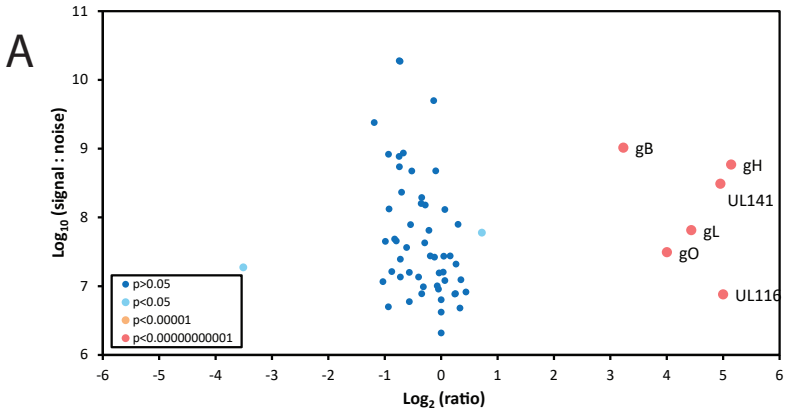
A
Log10 (signal : noise)
Log2 (ratio)
gB
gH
UL141
gL
gO
UL116
p>0.05
p<0.05
p<0.00001
p<0.00000000001

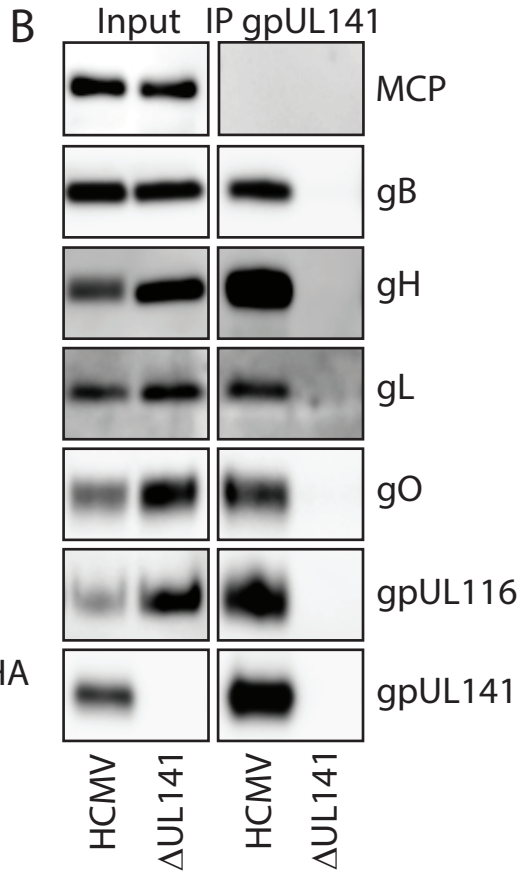
B
Input
IP gpUL141
MCP
gB
gH
gL
gO
gpUL116
gpUL141
HCMV
ΔUL141
HCMV
ΔUL141

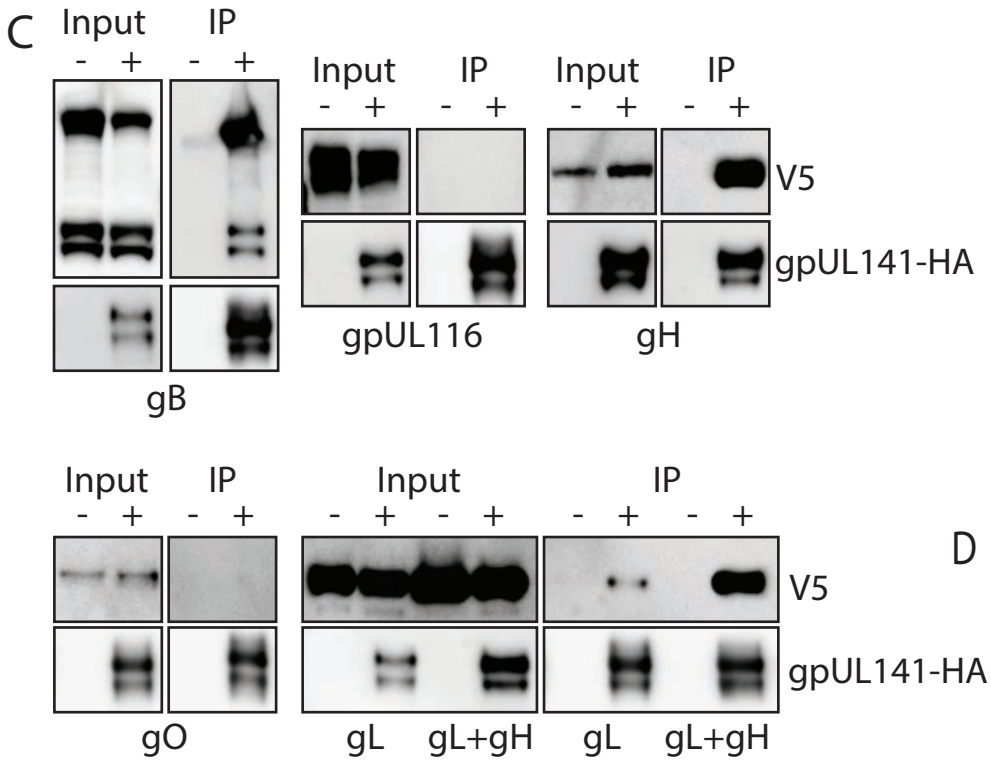
C
Input
IP
- +
- +
gB
Input
IP
- +
- +
gpUL116
Input
IP
- +
- +
gH
V5
gpUL141-HA
Input
IP
- +
- +
gO
Input
IP
- +
- +
- +
- +
gL
gL+gH
gL
gL+gH
V5
gpUL141-HA

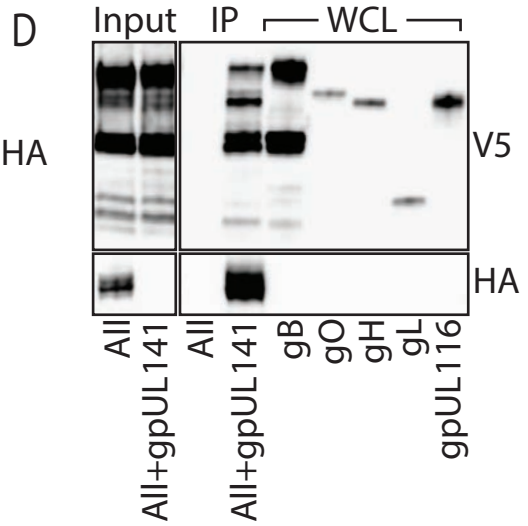
D
Input
IP
WCL
V5
HA
All
All+gpUL141
All
All+gpUL141
gB
gO
gH
gL
gpUL116

Figure 3

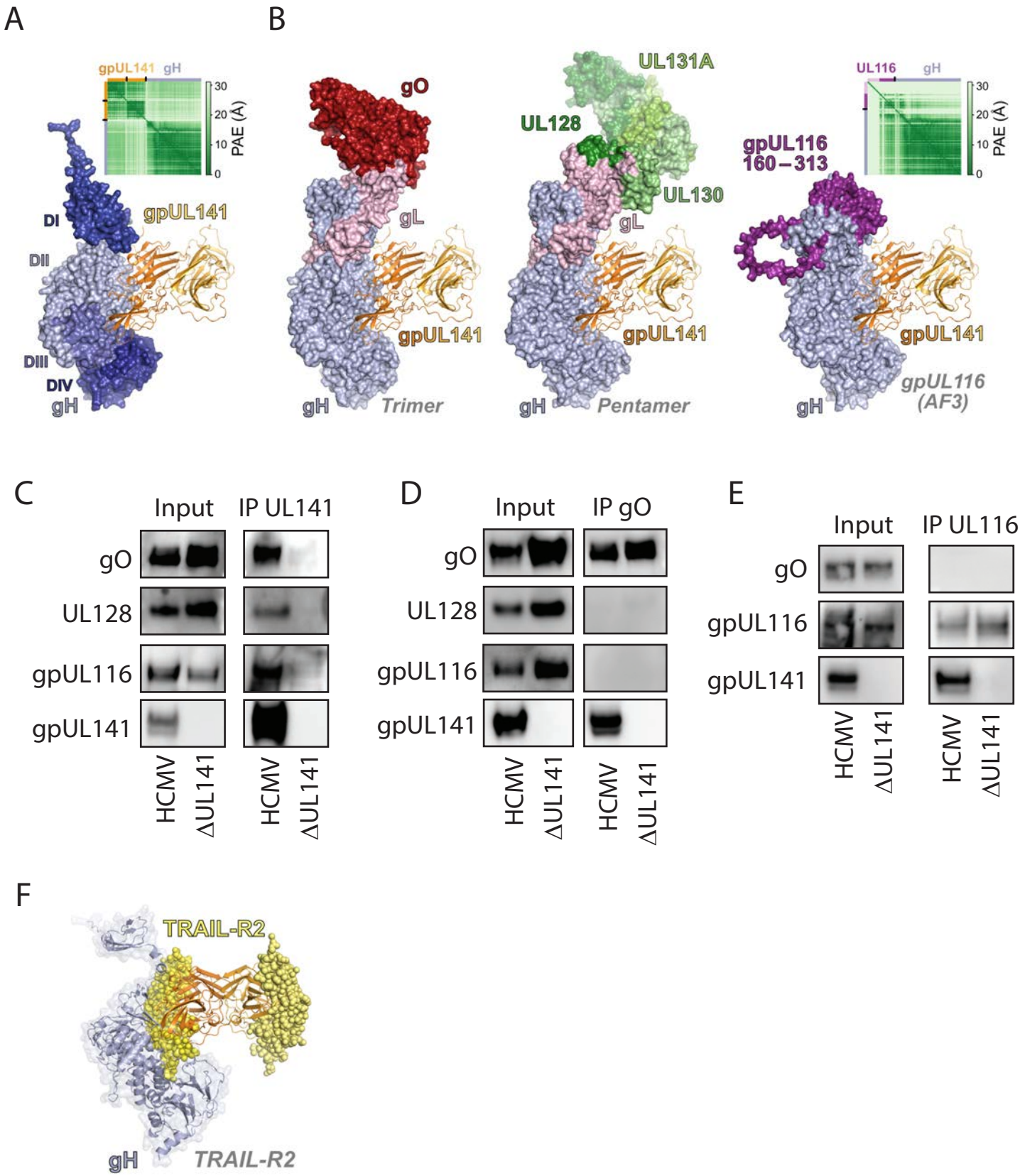
A
gpUL141
gH
30
20
10
0
PAE (Å)
DI
DII
DIII
DIV
gH
gpUL141
B
gO
gL
gpUL141
gH
Trimer
UL131A
UL128
UL130
gL
gpUL141
gH
Pentamer
UL116
gH
gpUL116
160–313
gpUL141
gH
gpUL116
(AF3)
C
Input
IP UL141
gO
UL128
gpUL116
gpUL141
HCMV
ΔUL141
HCMV
ΔUL141
D
Input
IP gO
gO
UL128
gpUL116
gpUL141
HCMV
ΔUL141
HCMV
ΔUL141
E
Input
IP UL116
gO
gpUL116
gpUL141
HCMV
ΔUL141
HCMV
ΔUL141
F
TRAIL-R2
gH
TRAIL-R2

Figure 4

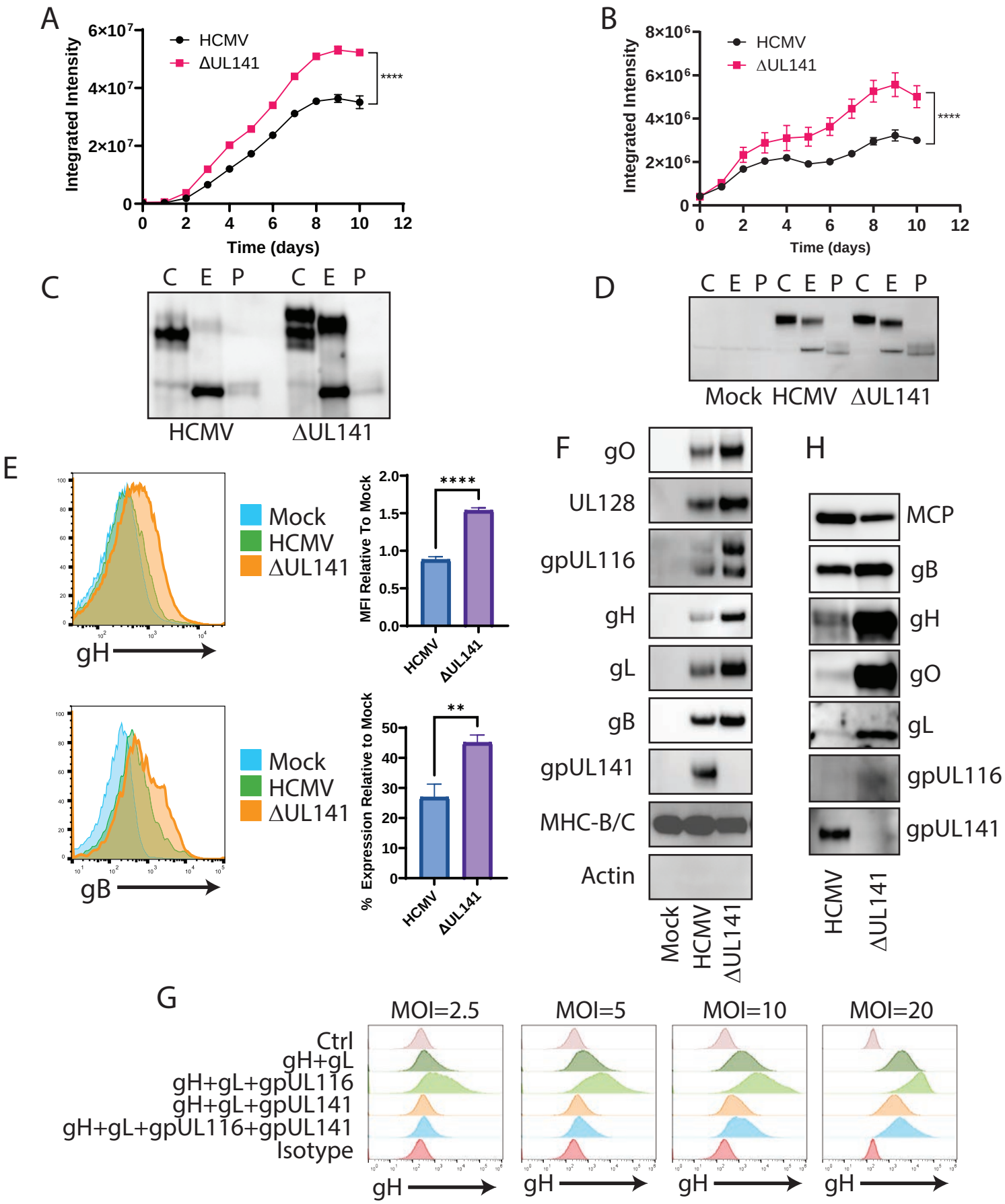
A
Integrated Intensity
6×10⁷
4×10⁷
2×10⁷
0
HCMV
ΔUL141
****
0 2 4 6 8 10 12
Time (days)
B
Integrated Intensity
8×10⁶
6×10⁶
4×10⁶
2×10⁶
0
HCMV
ΔUL141
****
0 2 4 6 8 10 12
Time (days)
C
C E P C E P
HCMV ΔUL141
D
C E P C E P C E P
Mock HCMV ΔUL141
E
Mock
HCMV
ΔUL141
gH
MFI Relative To Mock
2.0
1.5
1.0
0.5
0.0
****
HCMV
ΔUL141
Mock
HCMV
ΔUL141
gB
% Expression Relative to Mock
50
40
30
20
10
0
**
HCMV
ΔUL141
F
gO
UL128
gpUL116
gH
gL
gB
gpUL141
MHC-B/C
Actin
Mock
HCMV
ΔUL141
H
MCP
gB
gH
gO
gL
gpUL116
gpUL141
HCMV
ΔUL141
G
MOI=2.5
MOI=5
MOI=10
MOI=20
Ctrl
gH+gL
gH+gL+gpUL116
gH+gL+gpUL141
gH+gL+gpUL116+gpUL141
Isotype
gH

Figure 5

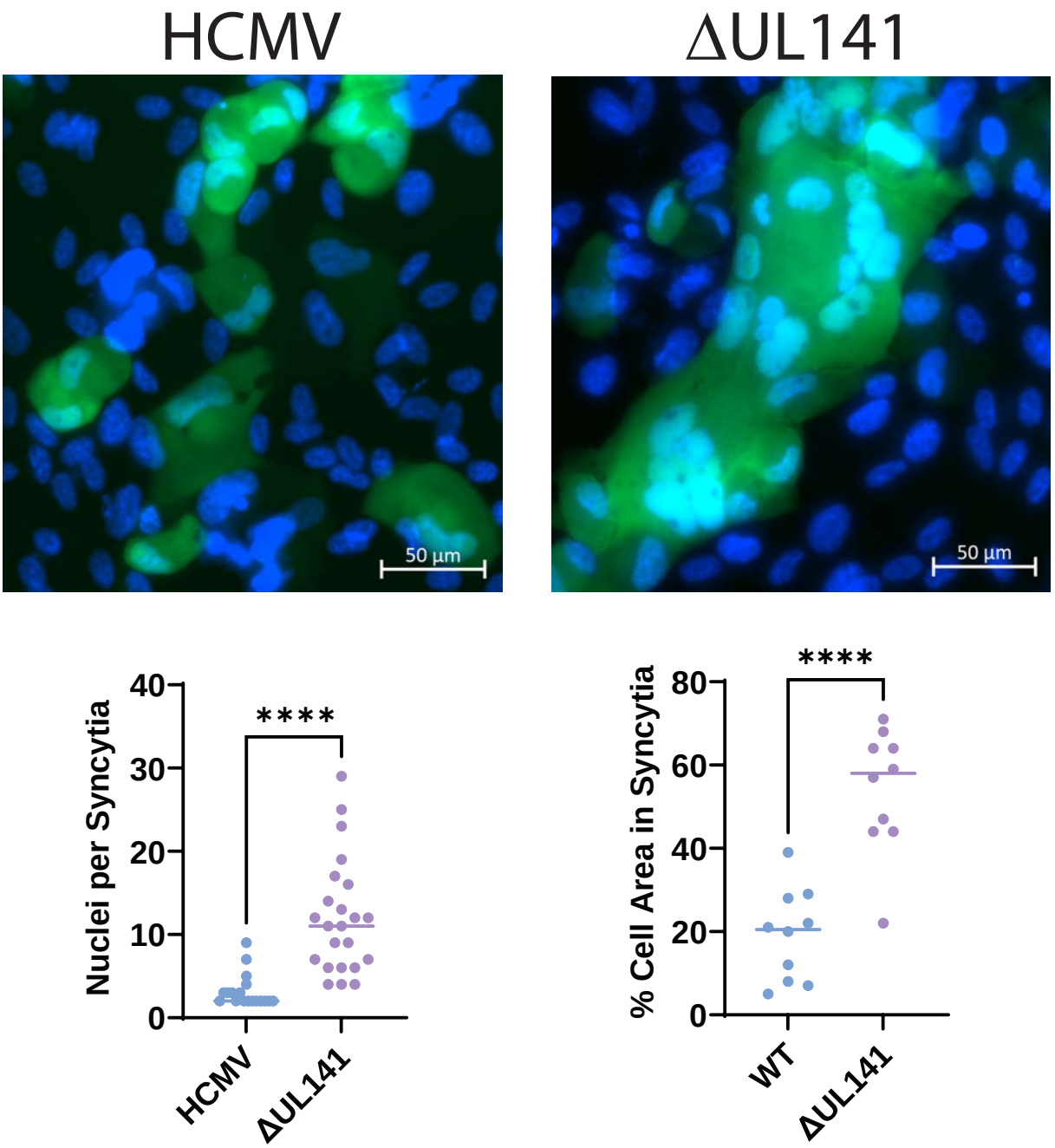
HCMV
ΔUL141
50 µm
50 µm
Nuclei per Syncytia
40
30
20
10
0
****
HCMV
ΔUL141
% Cell Area in Syncytia
80
60
40
20
0
****
WT
ΔUL141

Figure 6

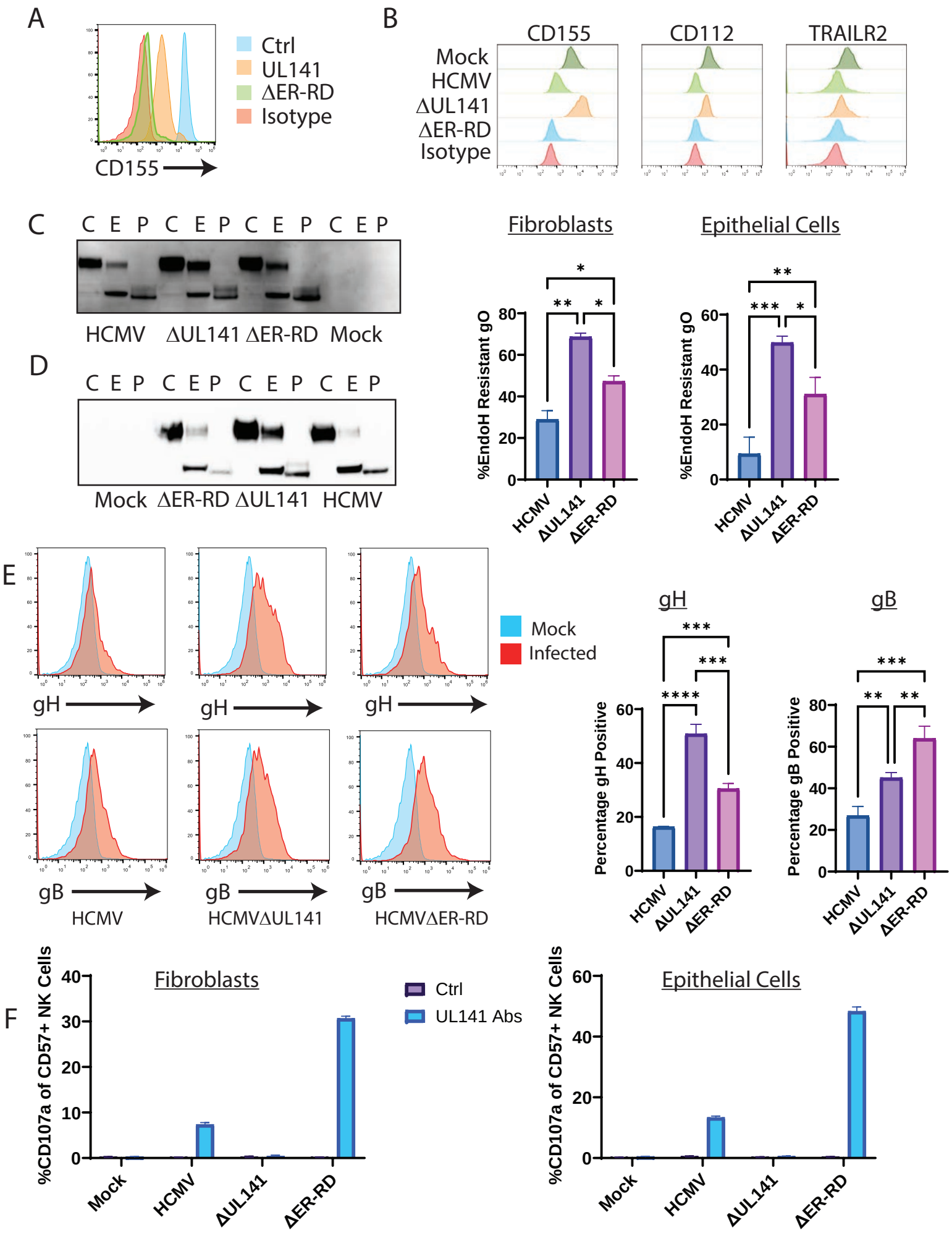
A
Ctrl
UL141
ΔER-RD
Isotype
CD155
B
CD155
CD112
TRAILR2
Mock
HCMV
ΔUL141
ΔER-RD
Isotype
C
C E P C E P C E P C E P
HCMV ΔUL141 ΔER-RD Mock
D
C E P C E P C E P C E P
Mock ΔER-RD ΔUL141 HCMV
Fibroblasts
Epithelial Cells
%EndoH Resistant gO
HCMV
ΔUL141
ΔER-RD
E
gH
gB
HCMV
HCMVΔUL141
HCMVΔER-RD
Mock
Infected
Percentage gH Positive
Percentage gB Positive
F
%CD107a of CD57+ NK Cells
Ctrl
UL141 Abs
Mock
HCMV
ΔUL141
ΔER-RD

Figure 7

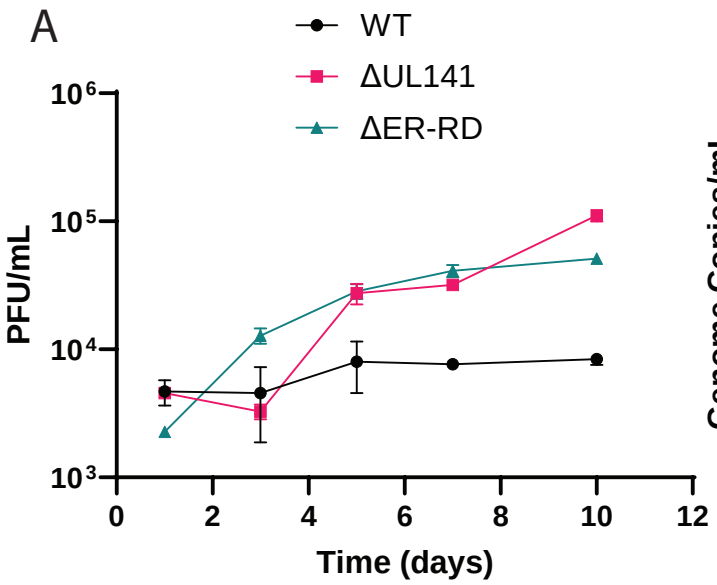
A
WT
ΔUL141
ΔER-RD
PFU/mL
10^6
10^5
10^4
10^3
0
2
4
6
8
10
12
Time (days)

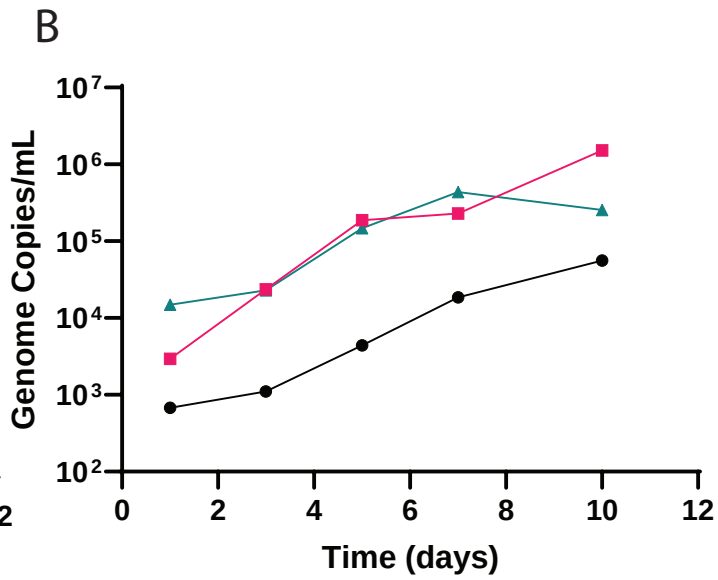
B
Genome Copies/mL
10^7
10^6
10^5
10^4
10^3
10^2
0
2
4
6
8
10
12
Time (days)

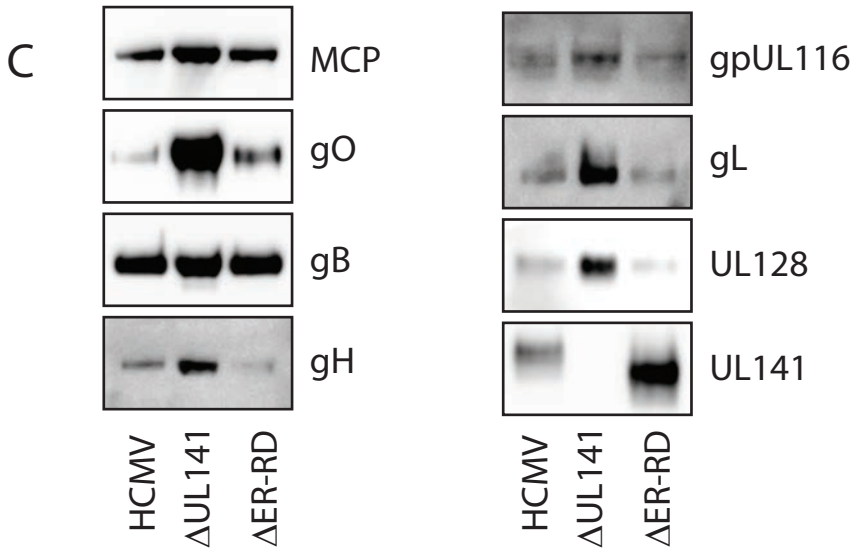
C
MCP
gO
gB
gH
HCMV
ΔUL141
ΔER-RD
gpUL116
gL
UL128
UL141
HCMV
ΔUL141
ΔER-RD

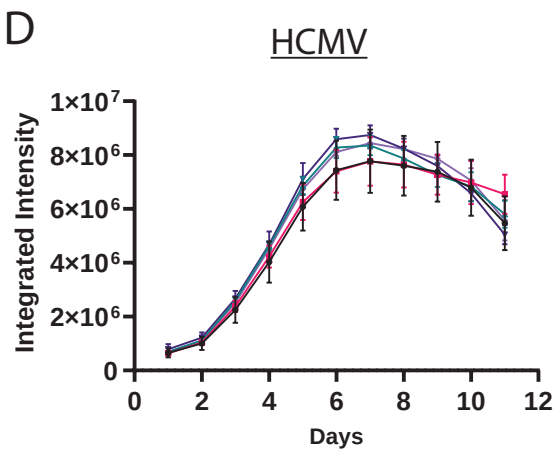
D
HCMV
Integrated Intensity
1×10^7
8×10^6
6×10^6
4×10^6
2×10^6
0
0
2
4
6
8
10
12
Days

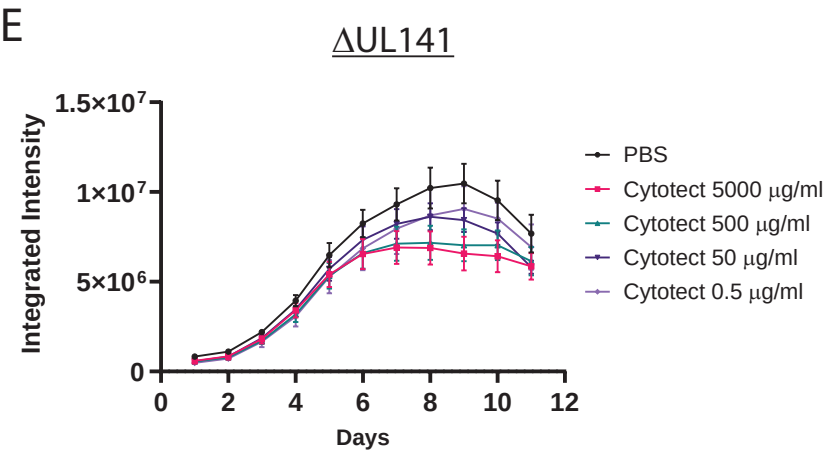
E
ΔUL141
Integrated Intensity
1.5×10^7
1×10^7
5×10^6
0
0
2
4
6
8
10
12
Days
PBS
Cytotect 5000 μg/ml
Cytotect 500 μg/ml
Cytotect 50 μg/ml
Cytotect 0.5 μg/ml

Figure Legends

Figure 1. gpUL141 is a novel virion envelope component, but does not lead to inhibition of NK activation in the virion. (A) Schematic of virions analysed in this study. (B) Virions from the passaged AD169 strain, or the wildtype Merlin strain, were purified from HFFF and analysed by Western blot. (C) Virions from strain Merlin were purified from HFFF then treated with detergent to extract membrane proteins, before assessing by Western blot. (D) Virions from strain Merlin were purified from HFFF then left untreated (E) or digested with EndoH (E) or PNGaseF (P) before analysing by Western blot. (E-F) cell-free strain Merlin virions were added to HFFF for 2h (E) or 24h (E), then cells co-incubated with NK cells for 5h in the presence of CD107a antibody and golgistop, before levels of NK-cell degranulation were assessed.

Figure 2. gpUL141 interacts with multiple entry glycoprotein complexes. (A) Cell-free strain Merlin virions that lacked UL128L but contained either a C-terminal V5 tag on gpUL141, or a deletion of UL141, were grown in HFFF in 'Medium' or 'Heavy' SILAC Media respectfully, then purified on glycerol-tartrate gradients and proteins subjected to IP with a V5 antibody. Samples were then analysed by MS, and the ratio of identified proteins between the two samples calculated. (B) Virions were prepared in the same way as (A) but without SILAC media, then analysed by Western blot. (C-D) RAd vectors expressing all potential gpUL141 interactors each with a C-terminal V5 tag, or gpUL141 with a C-terminal HA tag, were used to co-infect HFFF. (C) Each potential interactor was expressed alone (-) or with (+) gpUL141, then gpUL141 IP'd using an anti-HA antibody, before assessing by Western blot. (D) All interacting proteins were expressed together from RAds in the absence or presence of gpUL141, then IP performed for gpUL141, followed by Western blot analysis. To identify individual proteins in the mix based on size, whole-cell-lysates (WCL) of each protein expressed alone are provided alongside.

Figure 3. gpUL141 interacts independently with all major gH-containing glycoprotein complexes. (A) Predicted structure of gH (blue surface, coloured by domain) in complex with a homodimer of gpUL141 (orange ribbons). Inset shows the predicted aligned error (PAE) of the model. (B) Superposition of gpUL141 from the predicted gH:gpUL141 structure onto the electron cryo-microscopy structure of the trimer (PDB 7LBE[44], *left*), the crystal structure of the pentamer (PDB 5VOB[82], *middle*), and a predicted complex of gH with UL116 (*right*). For clarity, the N-terminal region of UL116 that is predicted to be highly unstructured is not shown. Inset shows the PAE of the gH:UL116 model. (C) HFFF were infected with strain Merlin containing either a C-terminal V5 tag on UL141, or a deletion of UL141, for 96h then proteins subjected to IP with an anti-V5 antibody followed by western blot. (D) HFFF were infected with strain Merlin containing or lacking UL141 expression for 96h, then proteins subjected to IP with an anti-gO antibody followed by western blot. (E) HFFF were infected with strain Merlin expressing a C-terminal HA tag on gpUL116 and either containing or lacking gpUL141 expression for 96h, then proteins subjected to IP with an anti-HA antibody followed by western blot. (F) Superposition of the predicted gH (blue semi-transparent surface and ribbons) plus gpUL141 (orange ribbons) complex onto the crystal structure of gpUL141 in complex with the death receptor TRAIL-R2 (yellow spheres; PDB 4I9X[12]).

Figure 4. gpUL141 alters the glycoprotein composition of both the virion and the infected cell-surface. (A-B) HFFF were infected with strain Merlin-GFP with UL141 either intact or deleted, at high MOI. 72h later cells were co-cultured with RPE-1 (A) or HUVECs (B). Once the HFFF had lysed (192h), virus dissemination through the RPE-1 of HUVEC monolayer was assessed by incucyte. (C) RPE-1 cells were infected as in (A), 192h post-co-culture infected RPE-1 cells were subjected to digestion with EndoH (E) or PNGaseF (P), or left under control conditions (C), then analysed for gO protein by Western blot. (D) HFFF were infected at high MOI with strain Merlin containing or lacking UL141, then 96h later subjected to digestion with EndoH (E) or PNGaseF (P), or left under control conditions (C), and analysed for gO protein by Western blot. (E) HFFF were infected for 72h with strain Merlin containing or lacking gpUL141, then levels of gH and gB on the cell surface assessed by flow cytometry. (F) HFFF were infected for 72h at high MOI with strain Merlin containing or lacking UL141, then cell surface proteins isolated by Plasma-membrane profiling (PMP) followed by Western blot. (G) HFFF-CAR were infected with RAd vectors expressing the indicated proteins for 48h, then stained for cell surface gH levels and assessed by flow cytometry. In all cases RAd-UL141 was used at MOI=20, all other RAds were used at the indicated MOI. (H) HFFF were infected for 72h at high

MOI with strain Merlin either expressing or lacking gpUL141, then co-cultured with uninfected RPE-1 cells. Virus was allowed to disseminate through the RPE1 monolayer until 100% CPE was achieved, at which point virions were purified and analysed by Western blot.

Figure 5. gpUL141 expression limits syncytia formation. HFFF were infected for 72h at high MOI by HCMV strain Merlin expressing GFP and either containing or lacking gpUL141 expression, then co-cultured with uninfected ARPE19 cells. After a further 6 days nuclei of live cells were stained with Hoechst, imaged by microscopy, and the number of syncytia quantified.

Figure 6. The gpUL141 ER retention domain alters envelope glycoprotein trafficking. (A) HFFF-CAR were infected with RAd vectors expressing wildtype UL141 or UL141 in which the C-terminal intracellular portion (containing an ER-retention domain (ER-RD)) had been deleted, then 48h later were stained for cell-surface CD155 levels and analysed by flow cytometry. (B-F) Cells were infected with wildtype HCMV strain Merlin or virus lacking either the whole of gpUL141, or just the C-terminal intracellular portion of gpUL141 (ER-RD). (A) HFFF were infected for 72h and then stained with anti-UL141 antibodies (A) or anti-CD112, CD155, or TRAILR2 antibodies (B) and analysed by flow cytometry. (C) HFFF were infected for 96h or (D) HFFF were infected for 72h then co-cultured for uninfected RPE-1 cells for a further 8d, then samples subjected to digestion with EndoH (E) or PNGase F, or left undigested (C). (E) HFFF were infected for 96h then stained for cell surface gH or gB followed by flow cytometry. (F) HFFF were infected for 96h, alternatively HFFF were infected for 72h and then co-cultured with RPE-1 cells for 24h before infected RPE-1 cells were isolated by MACs, and left until 96h post co-culture. Infected cells were then co-cultured with NK cells for 5h in the presence of CD107a antibody and golgistop, before the percentage of degranulating NK cells were assessed.

Figure 7. gpUL141 alters virus growth, virion incorporation, and susceptibility to neutralising antibodies. (A-B) HFFF were infected for 72h at high MOI with wildtype HCMV strain Merlin-GFP or virus lacking UL141 then co-cultured with uninfected RPE-1 cells. xd later the supernatants were harvested and analysed for live virus by plaque assay (A) or encapsidated genomes by qPCR (B). (C) HFFF were infected for 72h with wildtype HCMV strain Merlin or virus lacking either the whole of gpUL141, or just the C-terminal intracellular portion of gpUL141, which contains a ER-retention domain (ER-RD). HFFF were co-cultured with RPE-1 cells and maintained until 100% CPE, at which point cell-free virions were purified and analysed by Western blot. (D-E) HFFF were infected for 72h with HCMV strain Merlin-GFP or the same virus lacking gpUL141, then added to uninfected HUVECs. Xd later the indicated concentrations of cytotect were added, and virus dissemination over time assessed by incucyte.

Supplementary Material

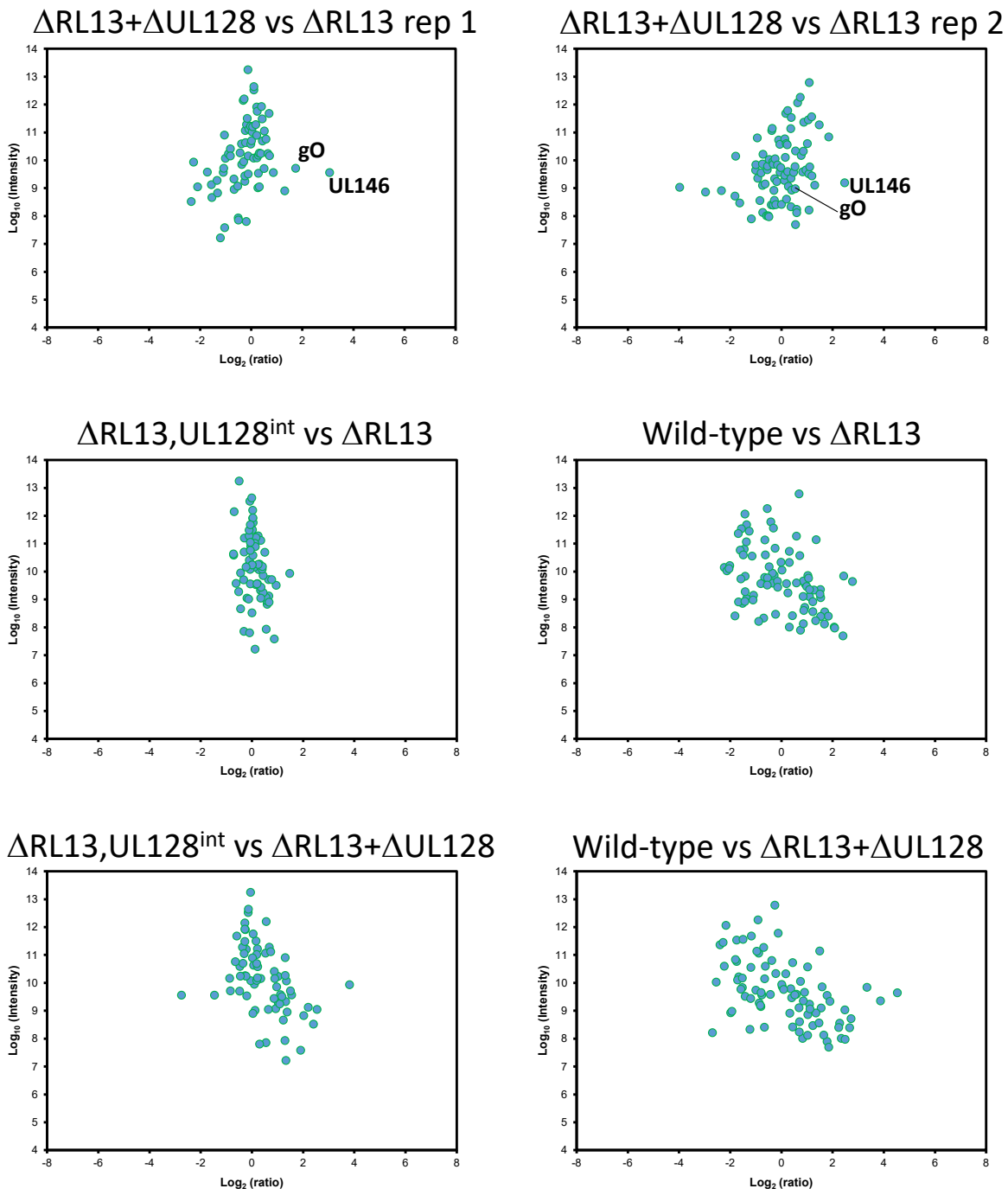

Figure S1: Scatter plot of viral proteins quantified in each SILAC-labelled virion experiment. The summed ion intensity (y axis) is shown as log10, and ratio (x-axis) as log2.

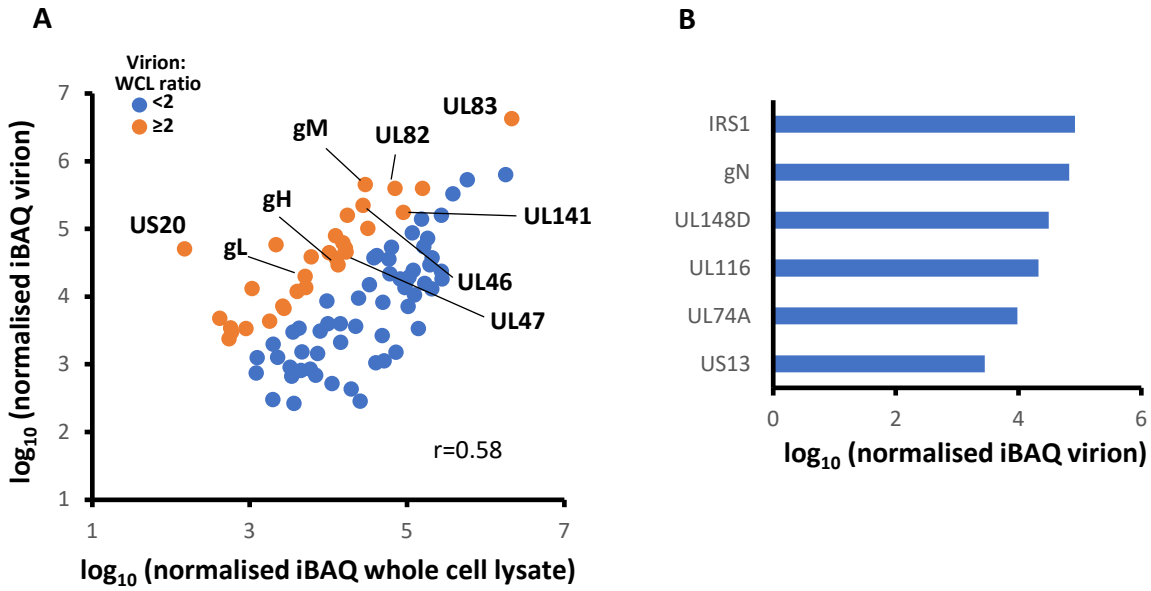

Figure S2: (A) comparison of abundance of HCMV proteins in the virion and in whole cell lysates (WCL) of infected cells. Proteins displayed in orange had a virion:WCL ratio of >2. (B) HCMV proteins only detected in the virion but not in WCL of infected cells. All proteins with a ratio of >1 are shown in Figure x and all quantified proteins are shown in Table S2.

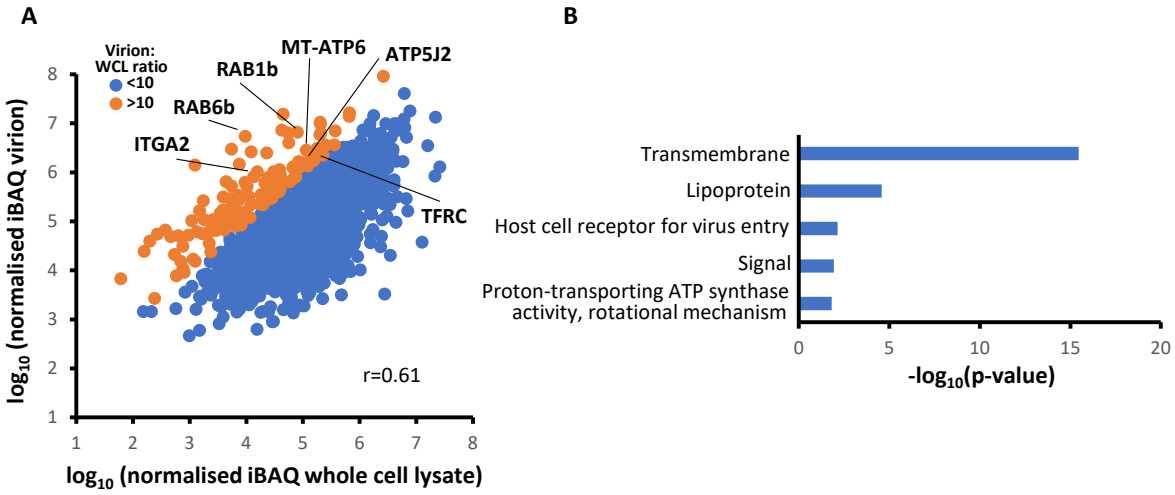

Figure S3: (A) comparison of abundance of human proteins in the virion and in whole cell lysates (WCL) of infected cells. Proteins displayed in orange had a virion:WCL ratio of >10. All quantified proteins are shown in Table S2B. (B) Enrichment of pathways within human proteins with a virion:WCL ratio of >2, using DAVID software, in comparison to all quantified human proteins. Full data are shown in Table S2C.

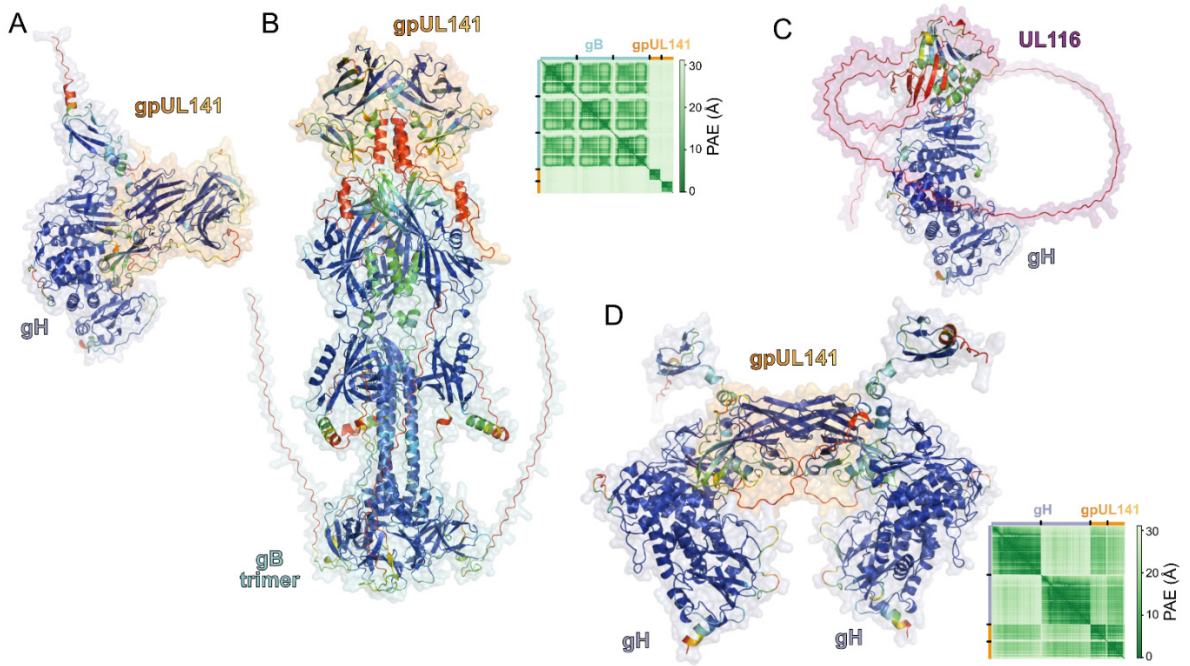

Figure S4. AlphaFold3 predictions of HCMV glycoprotein complexes. (A) Predicted structure of gH (blue semi-transparent surface) in complex with a homodimer of gpUL141 (orange semi-transparent surface). Proteins are shown as ribbons coloured by prediction confidence (predicted local distance difference test; pLDDT), from red (low confidence, pLDDT ≤ 50) to blue (high confidence, pLDDT ≥ 90). (B) Predicted complex between a homotrimer of gB (cyan semi-transparent surface) and a homodimer of gpUL141 (orange semi-transparent surface), with ribbons coloured as in (A). gB has been predicted in the post-fusion conformation[83]. Inset shows the predicted aligned error (PAE) of the complex, indicating low confidence in the orientation of gpUL141 relative to gB. (C) Predicted complex between a gH (blue semi-transparent surface) a UL116 (purple semi-transparent surface), with ribbons coloured as in (A). (D) Predicted structure of two gH molecules (blue semi-transparent surfaces) in complex with a homodimer of gpUL141 (orange semi-transparent surface). The PAE plot (inset) indicates that the relative orientations of gH molecules with respect to the gpUL141 homodimer are predicted with high confidence.